Modulation of dendritic AMPA receptors by different forms of synaptic plasticity

Thesis of Ph.D.

Dr. Bertalan K. Andrásfalvy

Supervisor: Gábor Tamás Ph.D

University of József Attila
Institute of Natural Science
Department of Zoology and Cellbiology
Szeged

2004

Contents

Introduction

In recent years our laboratory we have mostly been focusing on single principal neurons and investigating the electrophysiological properties to get a better and more detailed picture of the basic unit of neuronal networks. The chosen subject for our investigation was the CA1 pyramidal neuron from adult rat hippocampus, because of the many favorable properties including easy preparation access, well-described anatomical circuitry and the known importance of their function in basic memory processes.

The hippocampus is part of the limbic system and one of the most studied parts of the mammalian central nervous system (CNS). The importance of this part of the brain in certain memorial tasks and learning have been investigated since the 1950s when clinical studies revealed the lack of these functions in different injuries or surgical removals of the hippocampus (Scoville & Milner, 1957). The hippocampal formation includes several distinct areas; dentate gyrus, hippocampus, subiculum, pre- and parasubiculum and the entorhinal cortex (**Figure 1.**). Based on morphology the hippocampus can be divided into two major regions, one close to the dentate gyrus containing large cells (regio inferior) and a distal region containing smaller cells (regio superior), as Ramon y Cajal described. Nowadays, the terminology of Lorento de Nó is mostly used, who divided the hippocampus into four parts, from CA1 to CA4. CA1 is equivalent to the small cell containing region superior, which we were focusing on. The elaborated dendritic arbors of these neurons extend perpendicularly to the cell layer in both (apical and basal) directions. CA1 principle pyramidal neurons receive excitatory and inhibitory information from several sources. CA3 neurons form synapses on the apical dendrites located in stratum radiatum (S. R.) and oriens (S. O.) through Schaffer collaterals. In stratum lacunosum-moleculare (S. L.-M.) the distal apical dendrites are innervated by different subcortical regions (thalamus, amygdala) and the entorhinal cortex. Recurrent collaterals from CA1 neurons innervate the basal dendrites. Excitatory asymmetric synapses are formed onto cortical-like spines on the dendritic arbor of CA1 pyramidal cells. Inhibitory inputs come from the very diverse forms of GABAergic interneurons, including basket cells and 17 others (not shown) which have restricted target regions and no spines.

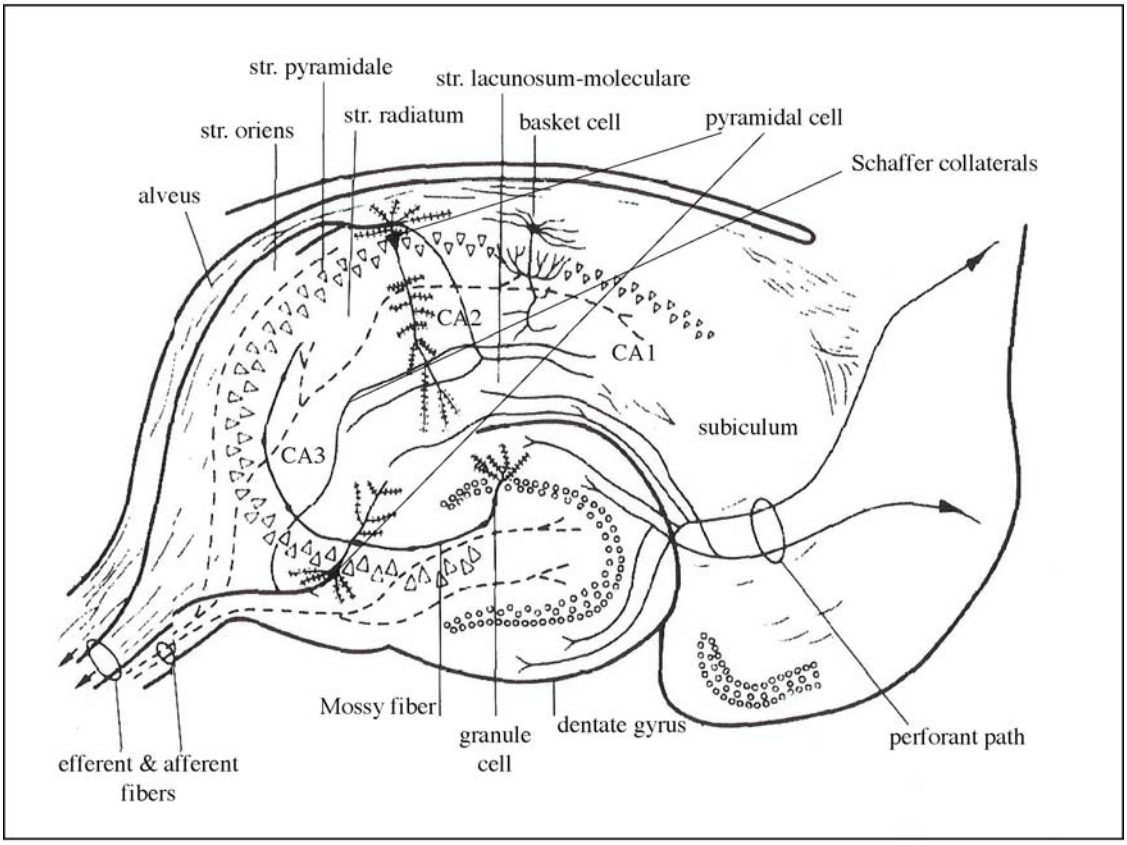

Figure 1. Schematic view of hippocampal cellular and network structure (see text).

CA1 pyramidal neurons have tens of thousands of excitatory and inhibitory synaptic connections with other neurons, and the integration of these thousands of inputs determins the electrical activity of the individual neuron. Information transfer through the synaptic connections is mainly mediated by two neurotransmitters: glutamate and γ-amino-butyric acid (GABA). The excitatory (glutamatergic) synaptic inputs are widely spread out over several hundreds of micrometers on the dendritic arbor, whereas the action potential output is localized at the proximal site of the axon. These excitatory synaptic transmissions are conveyed by, the glutamate activated ionotropic channels (iGluR) α-amino-3-hydroxy-5-methyl-isoxazole-4-propionate (AMPA), *N*-methyl-D-

aspartate (NMDA) and kainate (KA), which are named after the agonists that selectively stimulate them. These receptors are located in the postsynaptic membrane and activated by the presynaptically released glutamate. AMPA receptor mediated glutamate currents are responsible for the rapid information transfer between neurons, whereas the NMDA receptors have a detector function for specific patterns of activity which can induce long-term changes in the synaptic strength by modulating the AMPA responses. The released glutamate bindings to the AMPA receptors are enough to active them, whereas NMDA receptor activity needs glycine as a co-agonist, as well as simultaneous membrane depolarization to remove the voltage-dependent Mg^{2+} block.

The topology of iGluR subunits consists of a large extracellular amino-terminus, four membrane-associated domains with the second transmembrane domain (TM2) forming a re-entrant loop, and an intracellular C-terminus. AMPA receptors are tetrameric or pentameric ionotropic channels, built from subunits GluR1-4, (**Figure 2.**). These subunits can form certain types of heteromeric or homomeric channels. Recently, several details of transport and insertion of different types of heteromeric AMPA receptor have become evident including the different physiological roles of different subunits determined mostly by their C-termini (Shi S-H et al., 2001), and where different phosphorylation and transport protein (Song & Huganir, 2002) binding sites are located (**Figure 2.**).

Figure 2. Subunit-specific regulation of AMPA receptors. A) Schematic drawing of a single AMPA receptor in the plasma-membrane, showing glutamate binding sites and the trans-membrane domains of subunits. B) Detailed amino-acid chains of the C-terminus of different subunits, indicating the transportation/anchoring protein binding sites and the phosphorilation points, suggesting functional differences between subunits.

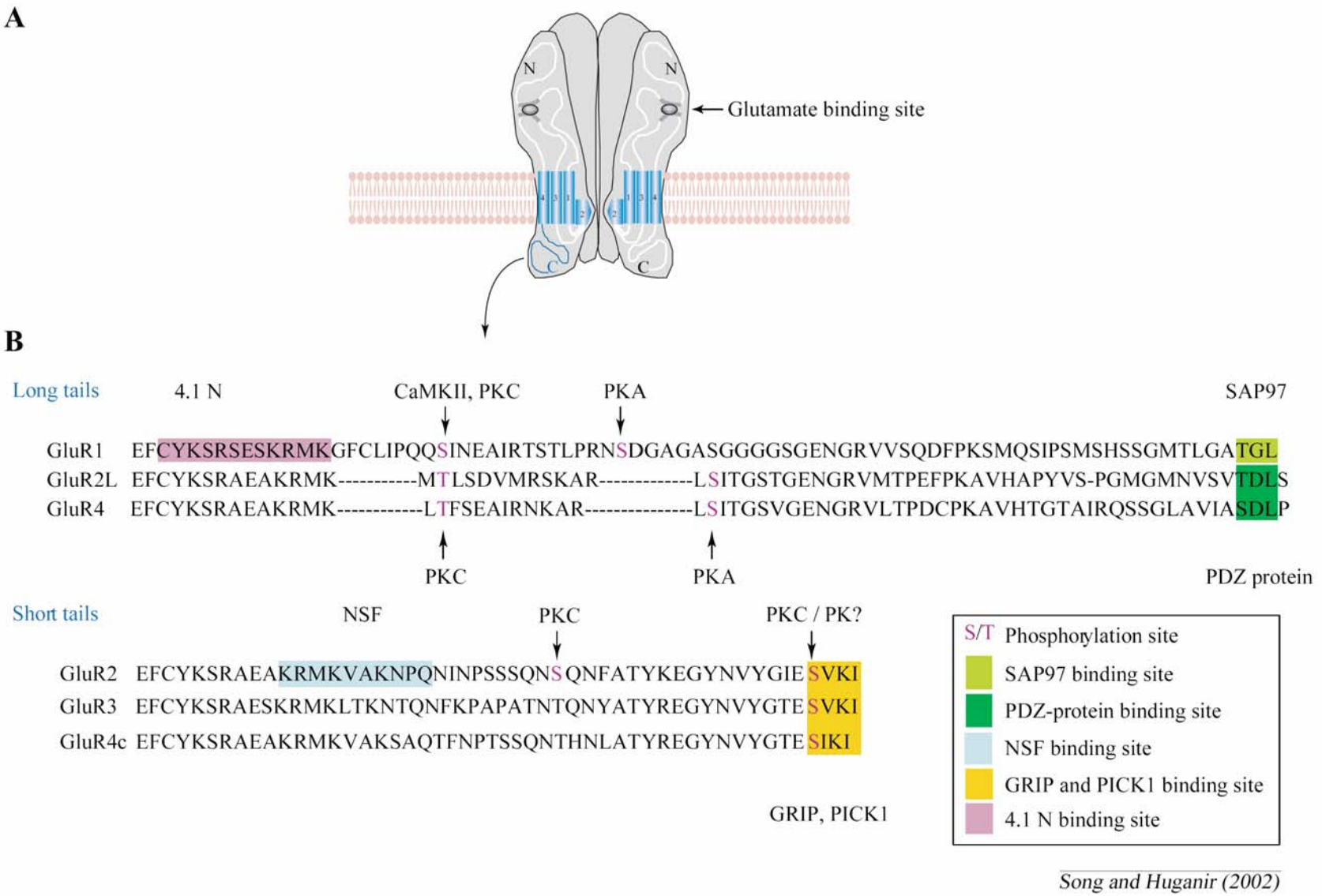

Song and Huganir (2002)

Recent studies strongly suggest that different subunit combinations of AMPA receptors are differentially involved in the three types of plasticity (I. Homeostatic, II. Hebbian-type and III. Distance-Dependent-Synaptic-Scaling) and offer a great opportunity to investigate them by manipulation of the receptor subunits.

I. Homeostatic plasticity provides network and cellular stability, globally optimizes synaptic connections and regulates excitability, adjusting gain of the neurons in dynamically changing environment

II. Hebbian type plasticity (LTP, LTD, etc) produces associative changes of individual synaptic strength and progressively modifies network properties increasing synaptic weight differences between synapses (depending on synaptic event history). It is believed to be crucial in computational tasks, learning and memory.

III. Distance dependent synaptic scaling (DDSS) adjusts the weight of every synapse to make them equally capable to have same impact on output regardless of their distance. Distance-dependent synaptic scaling (*DDSS*) (Magee & Cook, 2000; Magee, 2000; Andrásfalvy & Magee 2001; Smith et al., 2003; Andrásfalvy et al., 2003) shares many similar features with the two previously distinguished major forms of synaptic plasticity: *homeostatic* (Davis & Bezprozvanny, 2001) and *Hebbian* type (Turrigiano & Nelson, 2000). Like homeostatic plasticity, *DDSS* globally optimizes synaptic connections. The major target of all three forms of plasticity is the alteration of the level of synaptic transmission by changing the number and/or properties of postsynaptic glutamate receptors. H*omeostatic* plasticity globally alters the number of synaptic AMPA receptors by changing their half-life over minutes (Royer & Paré, 2003) or hours/days (O'Brien et al., 1998). *Hebbian* plasticity can change AMPA receptor number within minutes (Shi et al., 2001). The *DDSS* also works through increasing the number of AMPA receptors in proportion to the distance from the soma (Andrásfalvy & Magee 2001; Smith et al., 2003; Andrásfalvy et al., 2003).

Previous work suggested a strong relationship between different forms of synaptic plasticity and the density/properties of synaptically active glutamatergic and GABAergic receptors. In the last few years we have focused on DDSS and Hebbian-type plasticity to determine their underlying mechanisms. We have directly examined single synaptic transmission before and after different electrical/molecular manipulations in control and

genetically modified mice, avoiding the spatial and temporal influence of other synapses and/or anatomically uneven dendritic conductance differences that distort conventional somatic recordings. To characterize biophysical properties such as single-channel conductance, open probability, kinetic features and agonist affinity of glutamate-activated channels we used outside-out patches excised from dendrites. This provided insight into specific alterations of excitation in chemically and genetically manipulated rats and mice.

Part I.
Distance-Dependent Increase in AMPA Receptor Number in the Dendrites of Adult Hippocampal CA1 Pyramidal Neurons

In our investigation we focused on the apical dendrites of CA1 pyramidal neurons, innervated by the Schaffer collaterals coming from the CA3 neurons. The Schaffer collateral pathway provides hippocampal CA1 pyramidal cells with a fairly homogeneous excitatory synaptic input that is spread out across several hundred microns of their apical dendritic arborizations. A progressive increase in synaptic conductance, with distance from the soma, has been reported to reduce the location-dependence that should result from this arrangement. The thousands of excitatory synaptic contacts within this pathway primarily utilize AMPA- and NMDA-type glutamate receptors. One of the simplest ways that dendrites shape incoming activity is to reduce the amplitude and increase the width of EPSPs (Rall, 1962; Jack & Redman, 1971; Jaffe & Carnevale, 1999). Because the cable filtering properties of the dendrites are responsible for this transformation, the effect increases with the distance an EPSP propagates. In this case the impact of synaptic input would depend on the dendritic location of the active synapses, with more distant synapses having a blunted effect when compared to those located in more proximal regions. It has been recently reported, however, that unitary EPSP amplitude at the site of the synapse increases with distance from the soma and that this increase helps counterbalance some of the filtering effects of the dendrites (Stricker et al., 1996; Magee & Cook, 2000). The final result is that for Schaffer collateral input to

CA1 pyramidal cells, unitary EPSP amplitude at the soma does not show a marked dependence on the dendritic location of the activated synapse.

A progressive increase in unitary synaptic conductance appears to be primarily responsible for the increase in dendritic EPSP amplitude observed in CA1 pyramidal neurons (Stricker et al., 1996; Magee & Cook, 2000). Several other studies, in the hippocampus as well as in other CNS regions, have also reported synaptic efficacy to be relatively location-independent. These studies further suggest that an increase in synaptic conductance is the primary mechanism (Inasek & Redman, 1973; Stricker et al., 1996; Korn et al. 1993; Alvarez et al. 1997). Finally the distal apical dendrites of both neocortical and hippocampal pyramidal neurons have been found to be more sensitive to glutamate than the proximal dendrites (Frick et al., 1998; Pettit & Augustine, 2000).

To further investigate potential postsynaptic mechanisms underlying the increased synaptic conductance of distal synapses, we directly recorded from the site of input using outside-out patches made from dendritic regions receiving Schaffer collateral synaptic input. Rapid application of glutamate to excised patches was used to estimate various postsynaptic properties including, AMPA receptor numbers, affinity, single channel conductance, maximum open probability, channel kinetics and current-voltage relationships in hippocampal CA1 pyramidal neurons. While we found no evidence of any location dependence of AMPA receptor subunit composition or channel modulation we did observe a greater than two-fold increase in AMPA receptor numbers. The data suggest that distal synapses contain a larger number of postsynaptic AMPA receptors compared to proximal synapses and that this elevation in receptor number could participate in generating the distance-dependent increase in unitary synaptic conductance found in these cells.

Materials and Methods

I. Preparation and visualization of hippocampal slice

Hippocampal slices (400 μm) were prepared from 6-12 week-old Sprague-Dawley rats using previously described standard procedures (Magee, 1998). Experiments were conducted using an upright Ziess Axioscope fit with differential interference contrast (DIC) optics using infrared illumination. Patch pipettes (5-11MΩ) were pulled from

borosilicate glass (EN-1, Garner Glass Co., Claremont, California), and filled with an internal solution containing 140 mM $KMeSO_4$, 1 mM BAPTA, 10 mM HEPES, 4 mM NaCl, 0.28 mM $CaCl_2$, 4.0 mM Mg_2ATP, 0.3 mM $Tris_2GTP$ and 14 mM phosphocreatine (pH 7.3 with KOH). Currents were recorded in voltage-clamp mode using an Axopatch 200B amplifier, filtered at 2 kHz and digitized at 20 kHz using Igor Pro XOPs. The normal bath external solution contained 125 mM NaCl, 2.5 KCl, 1.25 mM NaH_2PO_4, 25 mM $NaHCO_3$, 2 mM $CaCl_2$, 1 mM $MgCl_2$, 25 mM dextrose, bubbled with 95% O_2 and 5% CO_2 at room temperature (pH 7.4). All neurons had resting potentials between -60 and –75 mV.

Formation and size estimation of dendritic patches

Outside-out patches were excised from apical dendrites to apical tufts (0-300 μm). Pipettes with a resistance of 5-11 MΩ had an estimated diameter tip of approximately 1.5-2 μm. Sodium channel density is relatively uniform along the dendrite (Magee & Johnston, 1995; Colbert & Johnston, 1996). Thus to examine whether the surface area of patches excised at different locations along the dendrite were the same, peak Na^+ current amplitudes were examined. Outside-out patches were held at –80 mV and membrane voltage stepped to –20 mV for 100 ms. Consistent with previous findings, sodium channel densities were independent of patch location (soma, 16.07 ± 3.03 pA; 125 μm, 20.27 ± 4.85 pA; 250 μm, 17.5 ± 5.05 pA) indicating that patch size was roughly uniform.

Fast application

Fast application of agonist was performed as previously described (Colquhoun et al., 1992). Briefly, double-barreled application pipettes were fabricated from theta glass tubing and solutions were perfused through control and agonist barrels at a rate of about 0.3 ml min^{-1} by means of a multi-lined peristaltic pump. The puffer external contains 125 mM NaCl, 2.5 mM KCl, 1.25 mM NaH_2PO_4, 10 mM HEPES, 2.5 mM $CaCl_2$ and 50 mM dextrose (pH 7.4). The 20-80% exchange times varied between 100-200 μs. Outside-out patches were placed in front of the control barrel. Movement of the application pipette, by means of a piezoelectric element, was used to apply agonist to the patch membrane.

After each patch recording, the application system was tested by breaking the patch and measuring the open tip current caused by a jump from a 10 to a 100 % puffer external solution. In addition, puffer solutions containing different concentrations of agonist and/or antagonist were exchanged using solenoid valves.

Estimation of synaptic versus extra-synaptic portion by electric stimulation

Afferent axons were stimulated by a tungsten bipolar electrode (A-M System, Carlsborg, Washington), located within 10-25 μm of the dendrite. Trains of 3-5 consecutive pulses at a frequency of 100 Hz were applied every 20 seconds for 10 minutes to stimulate glutamate release from adjacent nerve terminals. Synaptic stimulation was large enough to evoke several action potentials during the train. These experiments were performed at 34-35 ^{0}C to decrease glutamate spillover. In addition, the CA3 region of the hippocampus was removed to avoid spontaneous glutamate release and 10 μM bicuculline methiodide was added to the external bath solution. Furthermore, the bath external solution contained 1 mM Mg^{2+} to reduce spontaneous NMDA channel openings. Application of 20 μM MK-801 (RBI) to the bath external solution was used to block NMDA receptors that were gated by the stimulated synaptic activity. In addition, the effects of MK-801 were tested without electrical stimulation in the presence of 0.5 μM external TTX (RBI). To determine the amount of NMDA channel block, outside-out patches were excised from the stimulated region of the apical dendrite 10 minutes following MK-801 washout.

Data acquisition and analysis

Acquiring, analysis and fitting of data were performed using interactive programs (Igor Pro, Wavemetrics). AMPA current activation and deactivation were fit by single exponential function, whereas desensitization was best fit by double-exponential function. The rise times were determined as the time during which the current rises from 20 to 80% of the peak value. Patches showing rise times greater than 1 ms were assumed to have an improper patch configuration and were removed from analysis.

The concentration dependent relation for AMPA-activated peak current was determined using increasing concentrations of glutamate (10 μM to 10 mM) applied by 100 ms application pulse. Concentration-response data were fitted by the Hill equation:

$effect=effect_{max}/[1+(EC_{50}/c)^n]$,

where c is the agonist concentration, n the Hill coefficient, and EC_{50} the concentration where the half-maximal response was obtained.

Microscopic properties of AMPA channels were examined using non-stationary fluctuation analysis (Sigworth, 1980). AMPA currents were evoked every 2-3 s by a 1 ms pulse of 10 mM glutamate in the presence of 1 mM Mg^{2+}. Between 20 and 100 traces per patch were obtained for analysis. The mean variance (σ^2), determined from all responses, was plotted against the mean current for all responses. The plot was fitted with the function:

$\sigma^2=iI-(1/N)I^2+\sigma_b^2$

where, I is the total current and i is the single-channel current, N is the number of available channels in the patch and σ_b^2 is the variance of the background noise.

Single-channel conductance (γ) was determined as the chord conductance:

$\gamma=I(V_h-V_{rev})$

where V_h is the holding potential and V_{Rev} is assumed to be 0 mV.

The open probability (P_0) is determined by the equation;

$P_o=I/(i/N)$.

Numeric values are given as means ± standard error of the mean (S.E.M.). Error bars in the figures indicate standard error and are plotted only if they exceed the size of the symbol. Statistical significance was examined using Students t-test at the 5% level of confidence.

II. Hippocampal slices and synaptic currents in mice

Hippocampal slices (350 μm) were prepared from 42-54 day-old GluR1 -/- mice and wild type littermates (WT, C57BL6) using previously described standard procedures (Chen et al., 2001). Unless otherwise specified, the proximal recording location corresponds to a position were dendritic spine density had become substantial (50-75 μm from soma), and the distal location was a region approximately 30 μm from the termination of stratum radiatum (180-220 μm from soma, **Figure 13A,B**). Experiments were conducted using an

upright Ziess Axioscope microscope fit with differential interference contrast (DIC) optics using infrared illumination. Patch pipettes (5-8 MΩ) were pulled from borosilicate glass and filled with an internal solution containing in mM: 120 Cs-gluconate, 20 $CsCl_2$, 0.5 EGTA, 4 NaCl, 0.3 $CaCl_2$, 4 Mg_2ATP, 0.3 $Tris_2GTP$, 14 phosphocreatine and 10 Hepes (pH 7.2). The normal external solution contained 125 mM NaCl, 2.5 mM KCl, 1.25 mM NaH_2PO_4, 25 mM $NaHCO_3$, 2 mM $CaCl_2$, 1 mM $MgCl_2$, 25 mM dextrose, bubbled with 95% O_2 and 5% CO_2 at ~33 °C (pH 7.4). All neurons had resting potentials between -60 and –75 mV. Series resistances from dendritic whole-cell recordings were between 10 and 30 MΩ. Unitary synaptic events were evoked by pressure ejection of a hyperosmotic external solution (+300 mM sucrose), containing tetrodotoxin (TTX, 0.5 μM) and Hepes (10 mM) replacing $NaHCO_3$ (~700 mOsM). AMPA currents were isolated by the presence of external APV (50 μM) and (+)-bicuculline (10 μM). Currents were recorded at –70 mV using an Axopatch 200B amplifier, filtered at 5 kHz and digitized at 50 kHz.

Miniature EPSCs crossing an approximate 4 pA threshold level were selected for further examination using a template fit algorithm written in Igor Pro (Magee and Cook, 2000; Smith et al., 2003). Events were fit with a sum of two exponential functions to obtain peak amplitude, rise and decay time constants. Events that had rise-time constants greater than 400 μs were eliminated from analysis since these events were unlikely to be from local synapses (Magee & Cook, 2000). Amplitude histograms were constructed from between 50 and 200 (typically 100-150) unitary events and were fit with either a dual or triple Gaussian functions. Goodness of fit was determined from the chi-squared values for each function. In pair-pulse facilitation experiments, electric stimulation was applied with a tungsten bipolar electrode (A-M systems Inc., Carlsborg, WA) located ~20 μm adjacent to the dendrite, at first proximal, then at a distal position from soma.

Two-photon glutamate un-caging

For MNI-glutamate (MNI-glu) un-caging experiments, hippocampal CA1 pyramidal neurons were visualized using an upright Olympus BX50WI microscope (Olympus America, Melville, NY) fitted with a 100x, 1.0 NA water immersion objective as previously described (Smith et al., 2003). A mode-locked femtosecond- pulse Ti:sapphire

laser (Coherent Inc., Auburn, CA) was scanned with a modified confocal scan head (FluoView, Olympus America) and gated with a mechanical shutter at 4 ms (Uniblitz, Rochester, NY). Hippocampal slices were incubated in the standard external solution in the presence of TTX (0.5 μM), APV (50 μM) and ascorbate (2 mM). Whole-cell dendritic recordings were made using patch pipettes containing a Ca^{2+} free standard Cs-gluconate solution in the presence of ascorbate (2 mM) and bis-fura (150 μM; Molecular Probes Inc., Eugene, OR) replacing EGTA. Dendrites were voltage-clamped at -70 mV using an Axopatch 1D amplifier (Axon Instruments) and had access resistances of 15-30 MΩ. In addition, a broken pipette containing the standard external solution in the presence of TTX (0.5 μM), APV (50 μM), ascorbate (2 mM), CTZ (100 μM) and caged MNI-glu (12 mM) was position above the slice at the site of the recording electrode. All spines examined were between 20-30 μm below the surface of the slice.

The point spread function of focal volume for two-photon excitation, estimated using 0.1 μm fluorescent beads, was 0.34 μm laterally and 1.4 μm axially (full width half maximum; FWHM). The FWHM of glutamate current amplitude distributions obtained by point un-caging of MNI-glu (720 nm, 7 mW) at different locations (~0.16 μm lateral and 0.5 μm axial steps) on well-isolated spines was 0.6 μm laterally and 2.0 μm axially. Isolated spines were identified on the basis that no other spine was within 1 μm of the examined spine in the same lateral plane and no other spine was directly below or above this perimeter (Smith et al., 2003). For spines showing a head diameter greater than 0.4 μm, head volume was estimated directly from the spine head diameter determined from fluorescence point spread functions (FWHM) and substituted in the equation for a sphere; Volume $=(4\pi r^3)/3$ where r is the spine head radius. For spines with a smaller diameter, volume was estimated by referencing total fluorescence of the spine head acquired from three-dimensional reconstructions to the total fluorescence of a large (> 0.4 μm) spine head whose volume could be estimated as above (Smith et al., 2003).

III. Hippocampal slices from rat

Hippocampal slices (400 μm) were prepared from 8-12 week-old Sprague Dawley rats using standard procedures as described at the beginning of Material and Methods. 50 μM

Spermine was added into all internal solution. The internal pipette solution for Ca/CaM experiments consisted of 140 mM $KMeSO_4$, 0.5 or 5mM EGTA, 10 mM HEPES, 4 mM NaCl, 1.5 or 6.2 mM $CaCl_2$, 4.0 mM MgATP, 0.3 mM $Tris_2GTP$, 2-10 μM calmodulin (CaM) 25μM of calcineurin autophosphorylation inhibitory protein (CaN-AIP) were added and 14 mM phosphocreatine (pH 7.25 with KOH). The calculated and measured free Ca^{2+} concentration was ~48-60 μM. The test stimulus was a short burst of 3 stimuli given at 100 Hz to the Schaffer collateral fibers via a Tungsten electrode positioned 20-30 μm from dendrite. A stimulus amplitude that was sufficient to initiate one or two action potentials (AP) was chosen. The average of three traces was used. 1 second long 100 Hz stimulation was given twice with a 30 second interval to potentiate the cell. A cell-attached recording electrode was used to measure synaptic efficacy before and after tetanus. The CA3 region was surgically removed and 20 μM Bicuculline was added to reduce inhibitory input during the stimulation. 50 μM APV and 10 μM MK-801 were added in "unpotentiated" condition. Dendritic outside-out patches were excised at a distance of ~200 μm distal to the soma. The fast application of agonist was performed as describe previously (Andrásfalvy & Magee, 2001).

Measuring synaptic efficacy using cell-attached patch recordings

So as to not disturb the local intracellular environment, we monitored the electrical activity with a cell-attached patch recording for 10-20 min before and 20-30 min after tetanus stimulation (Frick et al., 2004). Every 20 seconds we gave 3 test stimuli (100 Hz), that were large enough to evoke one or two action potentials (AP). The recorded capacitive currents were analyzed by two separate criteria to evaluate the change in synaptic efficacy. First, we measured the first spike latency from the beginning of the recorded trace, based on the notion that the increased synaptic efficacy increases the depolarization of the neuron, so it reaches the threshold earlier in time (**Figure 17**). Second, we used the capacitive current traces as a measure of the evoked excitatory-post-synaptic-potantial (EPSP). The underlying idea is that during the potentiation the evoked EPSP increased and the elevated rate of voltage change (dV/dt) causes an elevated capacitive current ($I_c=C_m$ * dV/dt, where C_m is patch capacitance). Indeed following potentiation the deflection increased after tetanus (274 ± 48%; n=11, **Figure 17**), while

the deflection remained unchanged if the potentiation failed or was intentionally blocked by NMDA channel inhibition 110 ± 6%; n=12, **Figure 17**).

Dendritic region receiving stimulation

Although it is impossible to be exact, we can coarsely estimate the region of the dendrite being stimulated by the large amplitude electrical stimulation based on the following assumptions: we stimulated an approximately 20 μm^3 volume of radiatum, 30 μm away from the dendrite and SC axons innervating a particular dendrite can approach it from as much as a 45° angle (Sorra & Harris, 1993). Given these estimates and the complicated branching pattern of CA1 dendrites it is possible that up to a 100 μm length of the apical dendrite would receive tetanized synaptic input during the large amplitude electrical stimulation. These values fit well with previous observations of subthreshold dendritic Ca^{2+} influx associated with electrical synaptic stimulation (Magee et al., 1995; Magee & Johnston, 1997).

Statistics

Numeric values are given as means ± standard error of the mean (S.E.M.). Error bars in the figures indicate standard error and are plotted only if they exceed the size of the symbol. Statistical significance was examined using one-way ANOVA followed by Tukeys posthoc test at the 5% and 1% level of confidence.

Result

AMPA current amplitude versus distance

Outside-out patches were excised (Jonas and Sakmann 1991; Spruston et al. 1995) from the apical dendrites of CA1 pyramidal neurons at various locations in stratum radiatum (S.R.), ranging from stratum pyramidale (S.P.) to the border of the perforant path in the stratum lacunosum-moleculare (S.L-M.). Dendrites within this region form spiny glutamatergic synapses with the axons of CA3 pyramidal neurons comprising the Schaffer collateral pathway. Patches were voltage-clamped at –80 mV and AMPA

currents were activated by 1 ms pulses of 1 mM glutamate using a rapid glutamate application system (Clements et al., 1992).

The peak amplitude of the AMPA current increased approximately threefold for patches excised from the soma compared to patches excised from distal regions (soma: 192 ± 52; dendrite ~ 250 μm: 566 ± 74 pA; $p<0.005$). Anatomical studies have shown that there are few spines, and therefore Schaffer collateral synapses, formed on the proximal portion of CA1 pyramidal neurons (soma to just less than 100 μm distal). At this point (~100 μm) spine density reaches a constant value that is maintained over the entire span of the Schaffer collateral input to the apical dendrites (1.27 ± 0.28 spine/μm^2). Therefore much of the initial increase in AMPA current from the soma to 100 μm distant can be the result of the increase in synapse density (Bannister & Larkman, 1995; Trommald et al., 1995). The remaining approximately two fold increase in dendritic AMPA current amplitude, however, occurs across dendritic regions that have a constant spine density (from 276 ± 42 pA at 100 μm to 566 ± 74 pA at 250 μm distal, $p<0.005$) (**Figure 3A**). The slight decrease in APMA current observed in the most distal patches (300 μm) is likely the result of these patches being in or near S.L-M where spine density has been observed to again decrease (0.60 ± 0.17 spine/μm^2).

We, therefore, observed an approximately two-fold increase in AMPA receptor current across the range of CA1 apical dendrite that receives a uniform density of Schaffer collateral input (**Figure 3B**). In general terms the increase in current amplitude could be the result of differences in the number of channels present in our patches or to differences in the properties of these channels. The experiments described below were designed to distinguish between these two possibilities.

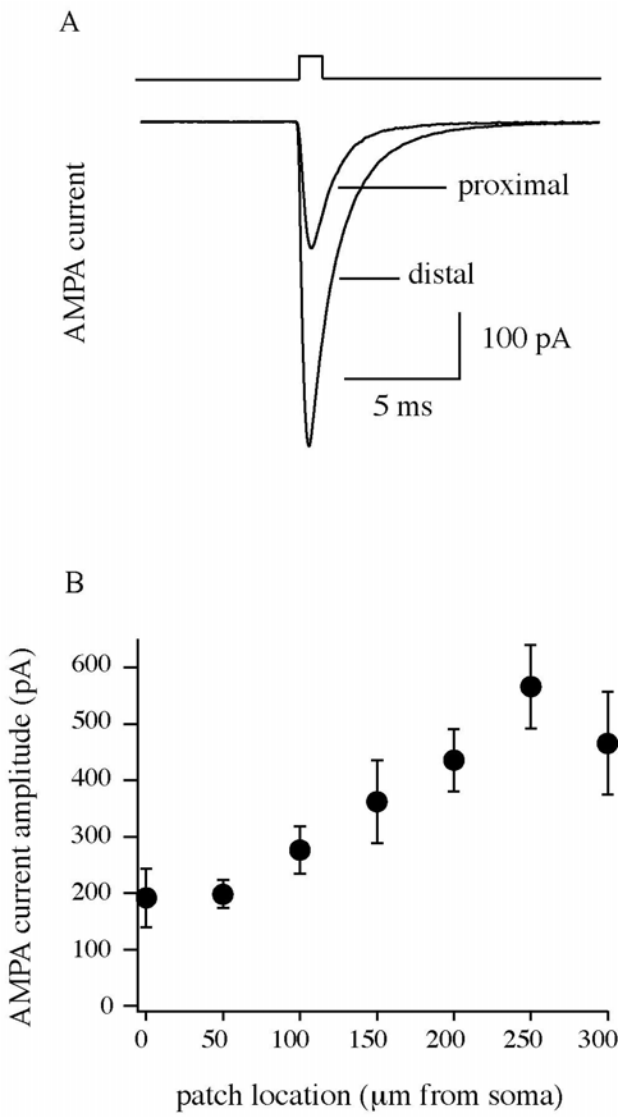

Figure 3. AMPA receptor-mediated glutamate currents in excised patches from different dendritic locations. **A)** Currents activated by 1 ms application of 1 mM glutamate to outside-out patches excised from either a proximal (~50 μm from soma) or distal (~250 μm from soma) dendritic location. Currents were recorded in the presence of 1 mM Mg^{2+} and in the absence of glycine. Each traces is an average of 5 sweeps (V_h was –80 mV). **B)** AMPA receptor-mediated mean current amplitudes are plotted against the location of the excised patches from the soma (n=69). Current amplitude increases approximately three fold across the range.

Agonist affinity

To determine if receptor glutamate affinity increased with distance from the soma, we examined dose-response relationships for AMPA-activated current from proximal and distal locations. Increasing concentrations of glutamate (10 μM to 10mM, 100ms pulse), were applied to patches excised from 50 μm and from 250 μm distal from soma. All peak current values were normalized to the peak responses (10 mM glutamate), and then plotted against concentration (**Figure 4A**). After being fit by a binding isotherm, dose-response curves did not show any significant shifts, with the EC_{50} of the proximal patches being equal to that of distal patches (436 μM (n=6) and 479 μM (n=7), respectively).

These data suggest that the agonist affinity of AMPA receptor is uniform with distance from the soma in CA1 pyramidal neurons.

Current voltage relationship

Differences in rectification or reversal potential can suggest possible AMPA receptor subunit composition change (Mosbacher et al. 1994). We determined the current-voltage (I-V) relationship of dendritic AMPA channels from outside-out patches excised at various locations along the dendrite. Patches were held at –80 mV and membrane voltage stepped up to +80 mV in 20 mV increments (**Figure 4B,C**). Peak currents were measured and normalized to the maximum current recorded at –80 mV. Proximal (50 μm) and distal (250 μm) AMPA currents displayed a linear I-V relationship and had reversal potentials of 4.2 ± 1.82 mV (n=4) and 4.4 ± 1.45 mV (n=6) respectively (**Figure 4D**). The slope conductance (G_m) of the proximally excised patches was 2.56 ± 0.44 nS, compared to 7.96 ± 1.68 nS for distal patches.

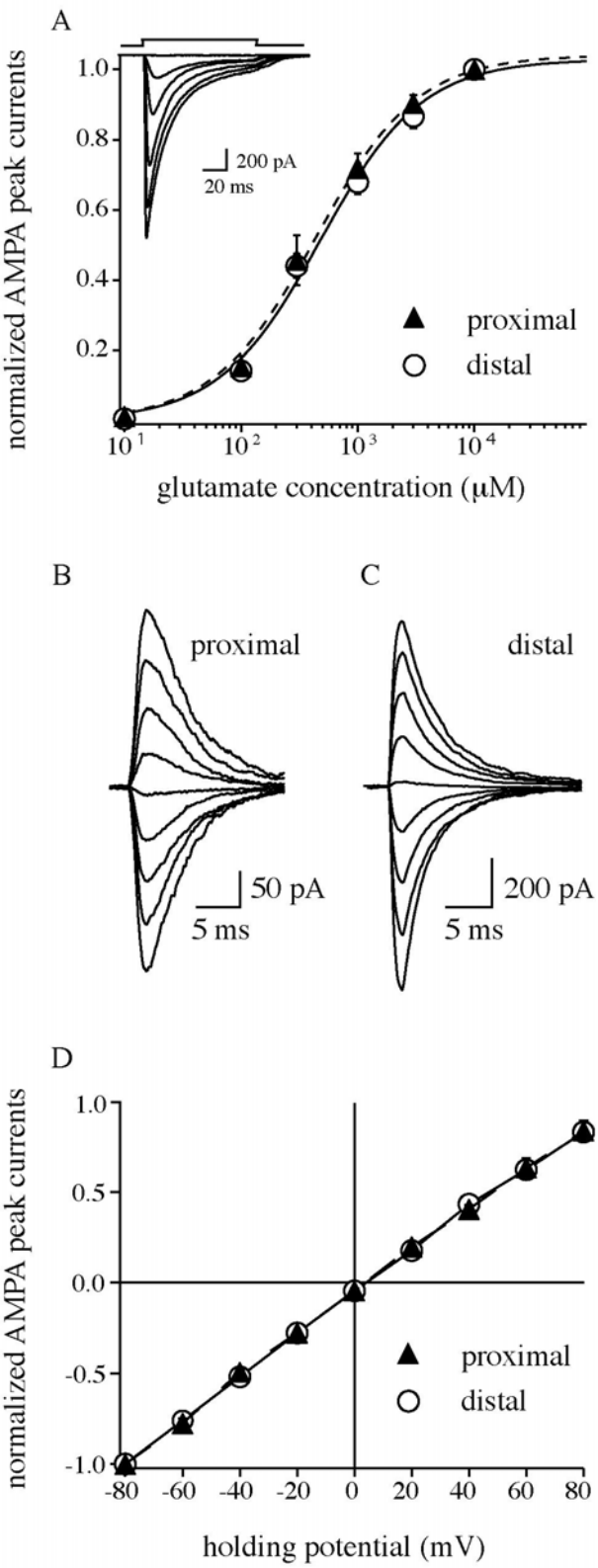

Figure 4. Agonist affinity and voltage-dependence of AMPA receptor-mediated glutamate current. **A)** Mean amplitude of AMPAR currents evoked by fast application of 10 to 10^4 μM glutamate with 100 ms pulses to proximal patches (~50 μm from soma, dash line with filled triangle, n=6) and distal patches (~250 μm from soma, solid line with open circle, n=7). Currents were normalized to the response at 10 mM glutamate. **B, C)** AMPA currents evoked by the application of 1mM glutamate for 1 ms (V_h was –80 to +80 mV, 20 mV steps) to proximal (**B**), and distal (**C**) excised patches. Each trace is a single sweep. **D)** Mean amplitude of AMPA currents for different holding potentials (V_h was –80 to +80 mV, 20 mV steps) during fast application of 1 mM glutamate for 1 ms to proximal (~50 μm from soma, dash line with filled triangle, n=5) and distal patches (~250 μm from soma, solid line with open circle, n=6). Currents were normalized to the response at –80 mV. In most cases the size of the symbols are bigger than the standard error bars. In all experiments, 0.1-1mM Mg^{2+} was added and no glycine.

Kinetics

Because the kinetic properties of AMPA receptor-mediated current are important for shaping glutamatergic EPSCs, we examined the location-dependence of AMPAR kinetics. The kinetic properties of the AMPA currents were studied using glutamate pulses ranging in duration from 1 to 100 ms. For all durations the currents rose rapidly to a peak and decayed within 10-20 ms, producing identical peak currents. The rise time of the current evoked by a 1 ms pulse of 1 mM glutamate could be fit by a single rising exponential, with a time constant of 0.58 ± 0.02 ms and a 20-80 % rise time of 0.47 ± 0.01 ms, across the dendrites (n=69, **Figure 5A**). The current deactivation could be fit by a single exponential, with a time constant of 2.8 ± 0.1 ms (Figure 5B) with no location-dependent differences observed across the somato-dendritic axis. During 100 ms 1 mM glutamate pulses, the current decayed with a double exponential time course having time constants of 7.6 ± 0.30 ms (τ_1, fast component, 90.3% ± 0.84, **Figure 5C**) and 25.69 ± 1.38 ms (τ_2, slow component, 9.7% ± 0.84, **Figure 5D**). There were no location-dependent differences in the desensitization kinetics or in ratio of fast and slow component observed (**Figure 5E**, $p>0.05$).

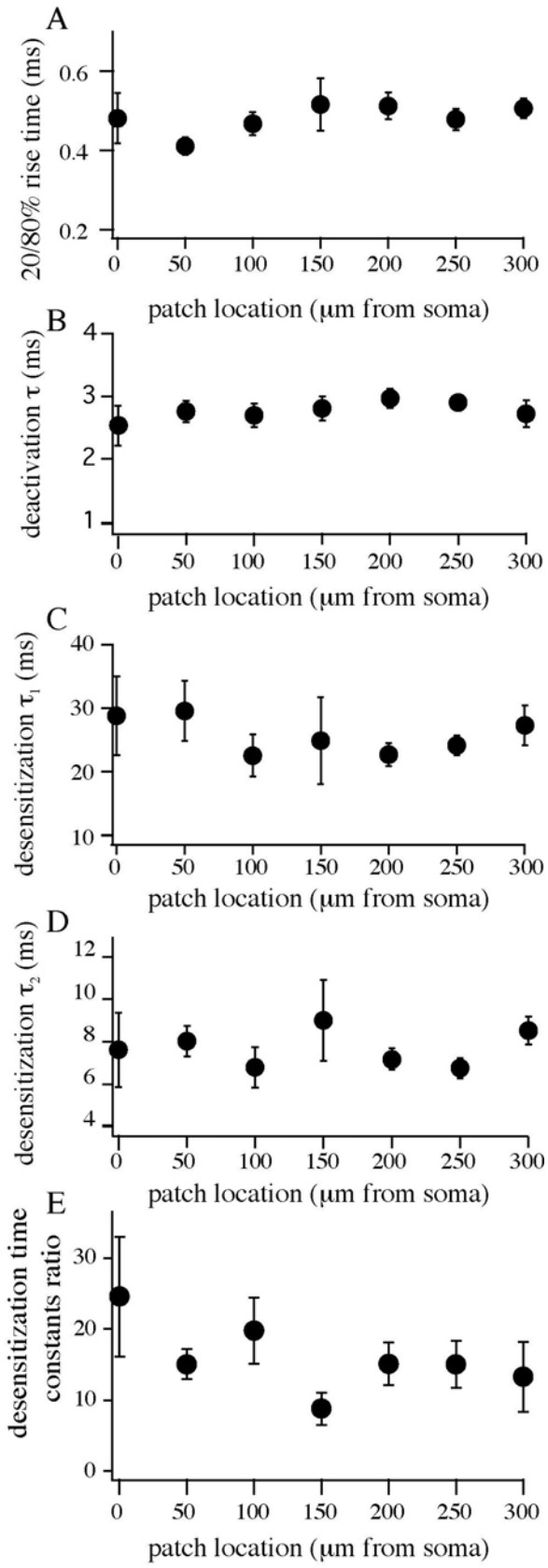

Figure 5. Kinetic properties of AMPAR mediated glutamate currents versus location. **A)** Mean of 20–80% rise time of AMPA current evoked by 1 ms application of 1mM glutamate on outside-out membrane patches excised from various locations of apical dendrites. **B)** Mean of deactivation time constants (τ) of the same AMPA currents evoked as in (A). **C)** Mean of fast desensitization time constants (τ_1) of AMPA currents evoked by 100 ms application of 1 mM glutamate to outside-out patches taken from various locations of apical dendrites. **D)** Mean of slow desensitization time constants (τ_2) of the same currents as in (C). **E)** Mean of the desensitization time constants ratio of AMPA currents shown in (B, C). In all experiments 0.1-1 mM Mg^{2+} was added with no additional glycine. In each figure, bars represent the standard error of the mean (n=69).

Concentration dependence of rise time and desensitization time course

The rise time and desensitization of glutamate activated AMPA current decreased in a concentration dependent manner. The 20 to 80 % rise time decreased with increasing glutamate concentration (1 ms pulses of 100 μM to 10 mM) from 1.9 ± 0.1 ms to values 0.2 ± 0.01 ms on patches excised from 50 μm from soma (n=6). The same decrease was seen from 2.1 ± 0.2 ms with 100 μM to values 0.2 ± 0.04 ms with 10 mM glutamate on patches excised from 250 μm (n=6, **Figure 6A**). The decay phase of the current (evoked by 100 ms pulses of 100 μM to 10 mM glutamate) traces was fit with the sum of two exponential functions. The predominant fast component, (τ_1) showed a concentration dependent decrease from 9.7 ± 1.5 ms with 100 μM glutamate to 6.6 ± 0.7 ms (n=12) with 10 mM glutamate. No difference was found in values between proximally (n=6) or distally (n=6) excised patches. The fast desensitization time constant was plotted against glutamate concentration from both locations together (**Figure 6B**).

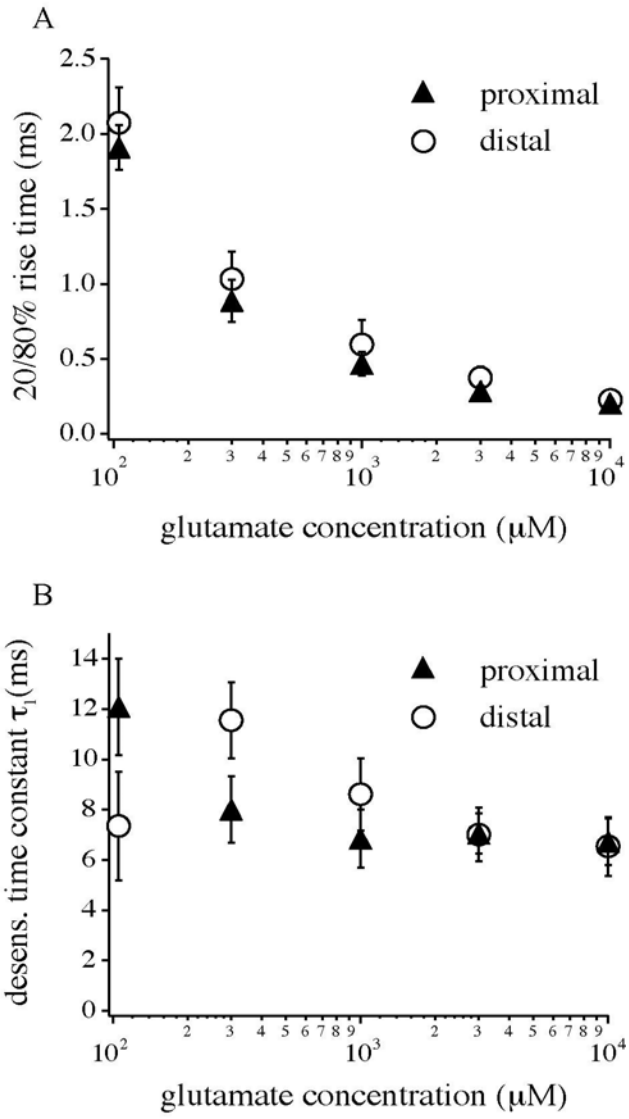

Figure 6. Concentration-dependence of AMPA current rise and desensitization

A) Concentration dependence of AMPA current 20-80% rise time for a 100 ms application of various concentrations of glutamate (100 to 10^4 μM). Data from proximal (~50 μm from soma, dash line with filled triangle, n=6) and distal patches (~250 μm from soma, solid line with open circle, n=6) are shown. Glutamate concentration is shown in log scale. **B)** Concentration dependence of the fast desensitization time constant (τ_1) with 100 ms application of glutamate for proximal (~50 μm from soma,

dash line with filled triangle, n=6) and distal patches (~250 μm from soma, solid line with open circle, n=6). Glutamate concentration is shown in log scale.

Non-stationary fluctuation analysis

We next examined several single-channel properties of dendritic AMPA receptor, namely the single-channel conductance and maximum open probability ($P_{o,max}$), to determine if there were any location-dependent differences. The single-channel conductance of AMPA channels (γ) was estimated using non-stationary fluctuation analysis of current evoked by 1 ms pulses of 10 mM glutamate (Sigworth, 1980). Between 20 and 100 traces per patches were obtained for analysis. The mean variance (σ^2), determined from all responses, was plotted against the mean current for all responses (**Figure 7A,B**). The plot was fit by a parabola (see Methods) to yield estimates of γ and the numbers of available channels (N). Data from 125 μm from the soma (n=4) and 250 μm from soma (n=5) resulted in similar values for γ of 9.83 ± 0.69 pS and 9.42 ± 0.95 pS respectively (**Figure 7C**). The probability of any given channel being open at the peak of the response ($P_{o,max}$) was also similar in both locations 0.83 ± 0.01 and 0.84 ± 0.02 respectively (**Figure 7C**). An approximately twofold increase in channel number was detected between the groups (N=467 ± 42, proximal 125 μm and N=1041 ± 206, distal 250 μm from soma, $p<0.05$, **Figure 7D**). These data, together with that described above, strongly suggest that the observed increase in AMPA current amplitude is the result of an increase in the number of channels present in the patch and not to any alteration in AMPA receptor properties.

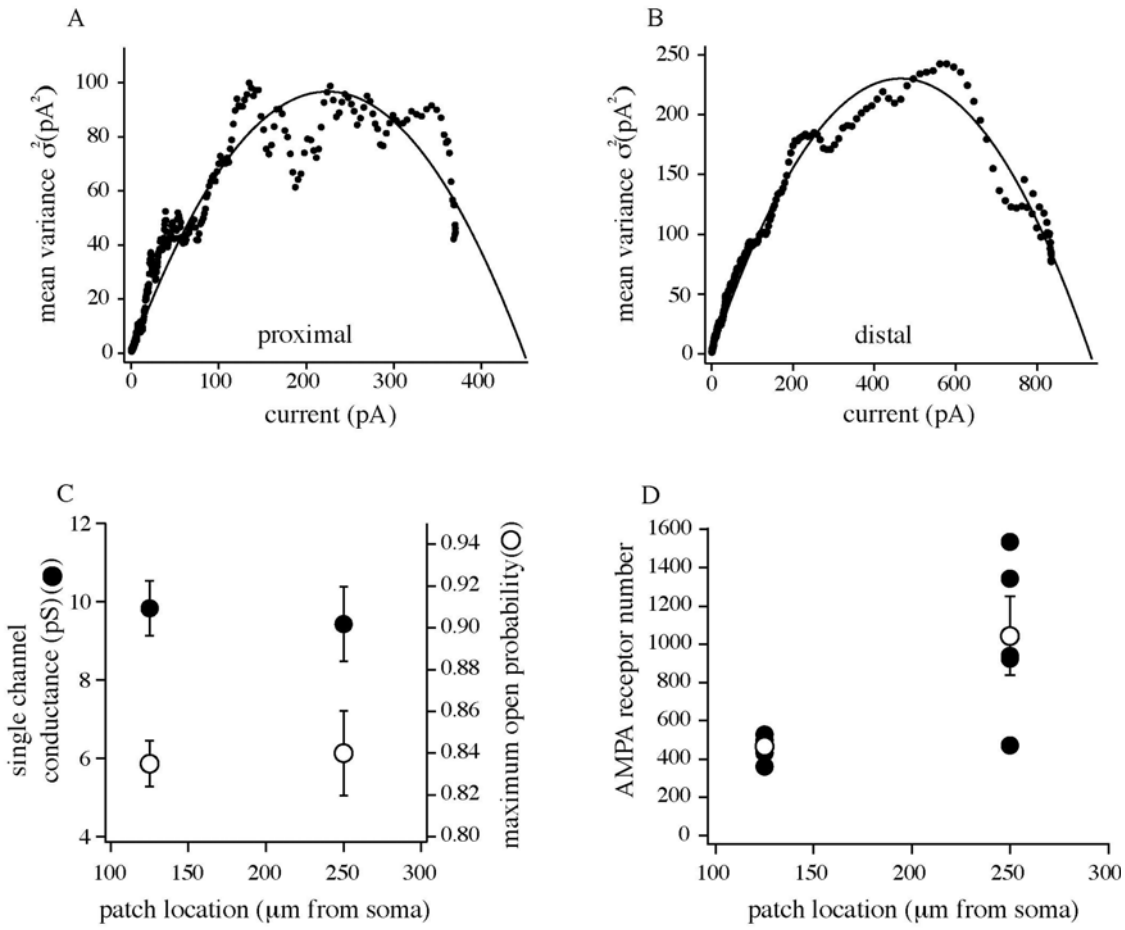

Figure 7. Non-stationary fluctuation analysis of AMPA receptor-mediated glutamate current. Mean variance plotted as a function of the mean current for a proximal **(A)** and distal **(B)** patch. Solid line is fit of the data by a parabolic equation (see Methods) that was used to determine single-channel conductance (γ), channel number (N) and maximum open-probability ($P_{o,max}$). Proximal patch from ~125 μm from soma and distal patch ~250 μm from soma. **C)** Single-channel conductance (left axis, filled circle) and maximum open-probability (right axis with open circle) versus location of the patches. Currents were evoked by a 1 ms application of 10 mM glutamate with 1 mM Mg^{2+} and in the absence of glycine. **D)** AMPA receptor number (N) versus patch location determined from the same patches as in (**C**). Filled circles are the N of single patches, open circle is the mean of these patches with standard error bars.

NMDA current amplitude versus distance

NMDA currents were activated on excised patches by 10 ms pulses of 1 mM glutamate in the presence of 10 μM glycine with 5 μM CNQX or 1 μM NBQX. The peak amplitude of

NMDA current does not change significantly with distance from the soma (**Figure 8A**) as NMDA currents from patches excised from the soma and distal dendrites (250 μm) had peak current amplitudes of 71.63 ± 19.35 pA and 52.33 ± 10.19 pA ($p>0.05$) respectively. Furthermore, dendritic NMDA currents do not change in patches excised at regions between 100 and 250 μm distal to the soma (54.34 ± 10.97 pA and 52.33 ± 10.19 pA, $p>0.05$, **Figure 8B**).

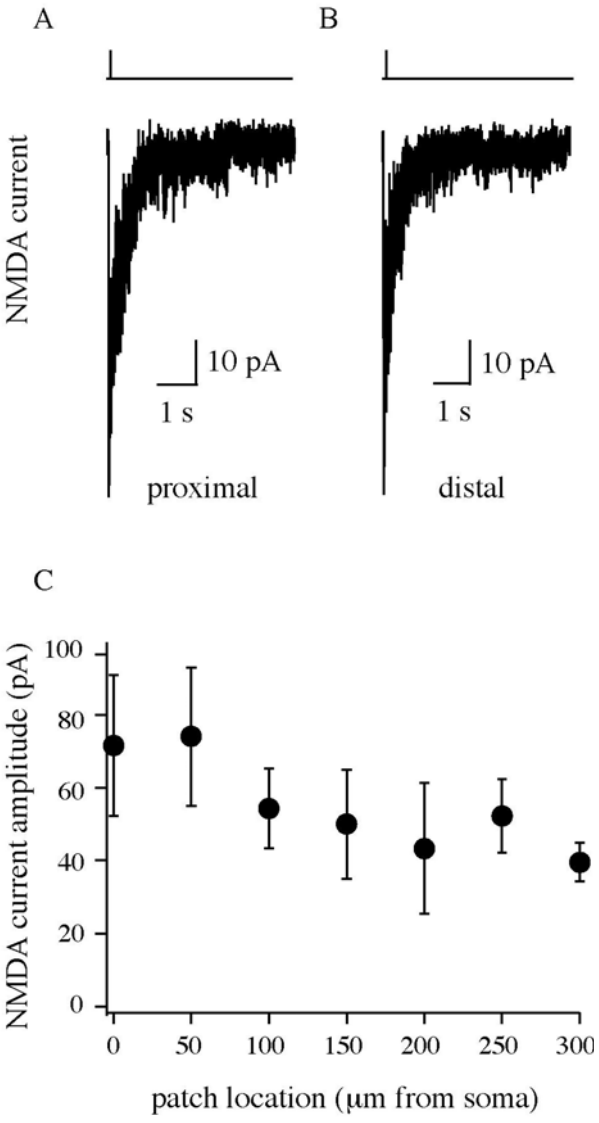

Figure 8. NMDA receptor-mediated glutamate currents in patches excised from different distances from soma. **A)** NMDA receptor mediated currents activated by a 10 ms pulse of 1 mM glutamate to either proximal (~50 μm from soma) or **B)** distal (~250 μm from soma) patches show the same amplitudes. Currents were recorded in the presence of 10 μM glycine and in the absence of Mg^{2+}. Each traces is an average of 5 sweeps (V_h was –80 mV). **C)** NMDA receptor-mediated mean current amplitudes are plotted against the location of the excised patches from soma on apical dendrite (n=60).

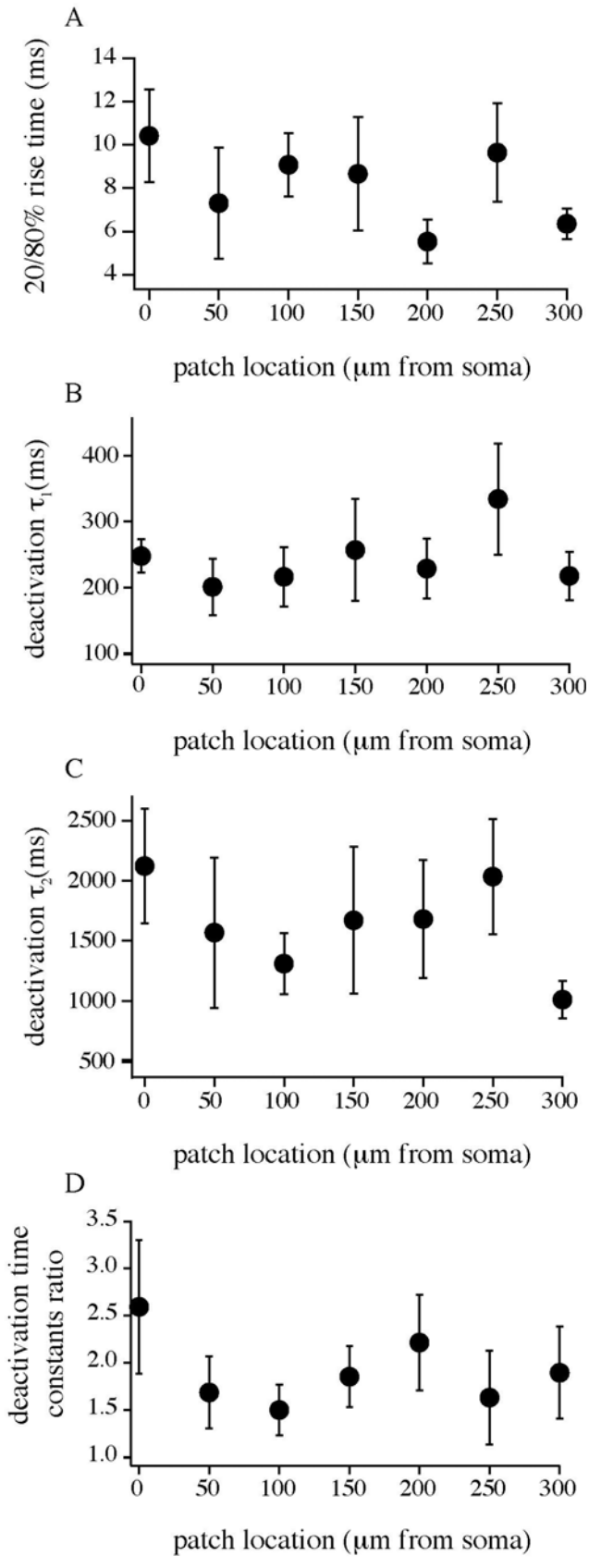

Figure 9. Kinetic properties of NMDAR mediated glutamate currents versus location. **A**) Mean of NMDA current 20–80% rise time for currents evoked by 10 ms application of 1mM glutamate to outside-out membrane patches excised from various locations of apical dendrites. **B**) Mean of fast deactivation time constants (τ_1) for NMDA currents evoked as in (**A**). **C**) Mean of slow deactivation time constants (τ_2) of NMDA currents as in (**A, B**). **D**) Mean of deactivation time constants ratio of the NMDA currents evoked as in (**B,C**). Currents were recorded in the presence of 10 μM glycine and in the absence of Mg^{2+}. Each traces is an average of 5 sweeps (V_h was –80 mV).

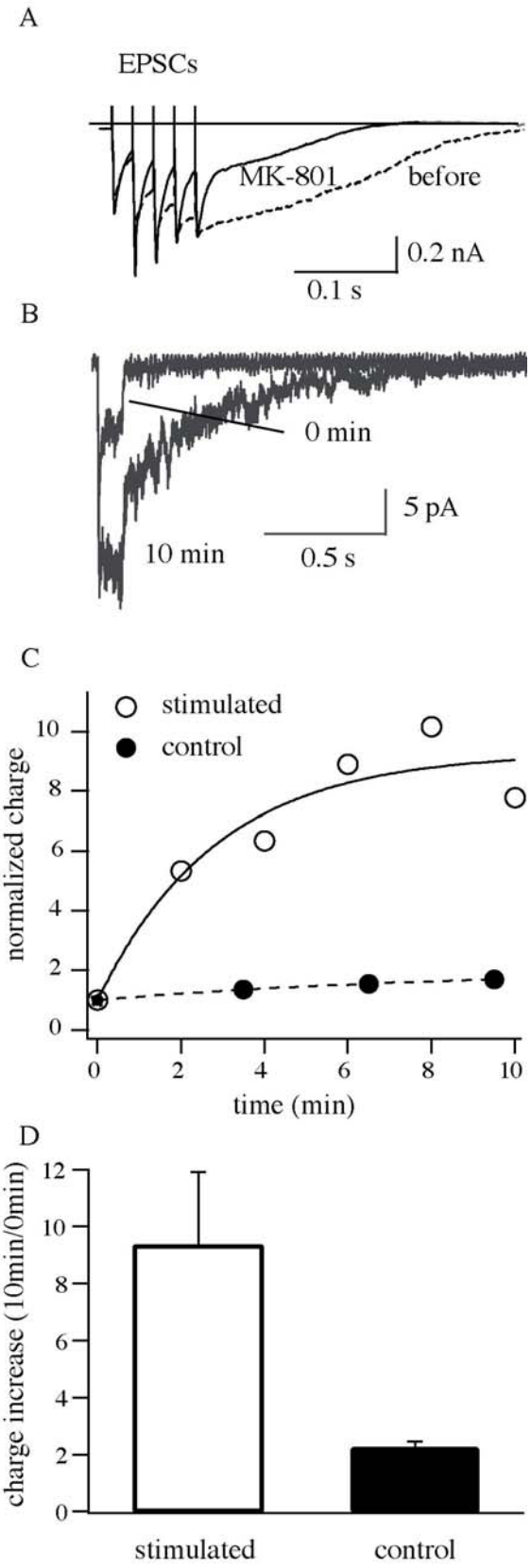

Figure 10. MK-801 block and recovery of synaptically-active NMDA receptors. **A)** Dendritic recording in whole cell mode, during electrically evoked EPSCs (see Methods). EPSC before (dashed line) and after (solid line) 10 minute bath application of 20 μM MK-801 during which synaptic stimulation was given every 20 seconds. The transient component of the EPSCs (primarily carried by AMPA receptors) did not change while the slow component (primarily carried by NMDA receptors) decreased significantly. Currents were recorded in the presence of 10 μM biccucculine, 1 mM Mg^{2+} and 0 mM added glycine. **B)** NMDA-mediated current evoked by 10 ms pulse of 1 mM glutamate to outside-out patches excised near the stimulating electrode (see Methods). Currents were recorded in the presence of 10 μM glycine and in the absence of Mg^{2+}. First trace shows a small NMDA current (0 min) because of little relief from MK-801 block. Ten minutes later (10 min) a much bigger current was detected as recovery had proceeded. To speed the recovery from block, patches were depolarized every second minute from –80 mV to +20 mV, and 3-4 glutamate pulses were applied for 500 ms (see Results). Each traces is an individual sweep (V_h was –80 mV). **C)** NMDA receptor mediated glutamate current evoked by 10 ms pulses of 1 mM glutamate current was integrated and normalized to the 0 min value and plotted against time. The charge increased rapidly with time during the relief of MK-801 block in the case of previous stimulation (open circle with solid line), while the control shows only a slight increase (filled circle with dash line). **D)** NMDA charge recorded after ten minutes divided by the charge of the first NMDA current (10min/0min) under control or test

conditions. NMDA charge increased approximately nine-fold in the stimulated cases (open bar, n=5) while in control only two-fold increase was observed (filled bar, n=6). This suggests that the majority of the glutamate receptors in outside-out patches are synaptic.

Kinetics

The kinetic properties of the NMDA current were studied using glutamate pulses ranging in duration from 1 ms to 3 s. For all duration applications the currents rose slowly to a peak within 5-20 ms, producing identical peak currents. The rise time course of the current evoked by a 1 mM, 10 ms glutamate pulse can be described by one rising exponential. The rising time constant was 6.46 ± 0.7 ms (data not shown) and the 20-80 % rise time was 8.58 ± 0.78 ms, across the dendrites (n=52, **Figure 9A**). The same current decayed with a double exponential time course having time constants of 252.5 ± 21.8 ms (τ_1, fast component, 61 ± 1.8%, **Figure 9B,D**) and 1.66 ± 0.15 s (τ_2, slow component, 39 ± 1.8%, **Figure 9C,D**). No location-dependent differences in the activation and deactivation kinetics of NMDA receptor-mediated currents ($p>0.05$,). To determine the time constant of desensitization, 3 s long glutamate pulses were used. From 27 patches 14 did not show any or very small desensitization and the decay could not be fit by an exponential function. In 13 cases the single exponential time constant was 760.26 ± 66.82 ms (data not shown).

Estimation of the proportion of synaptic receptors

It is likely that our patches contain a mix of synaptic and extra-synaptic receptors. Therefore we used the "irreversible" activity-dependent NMDA receptor blocker, MK-801 to determine the relative amount of synaptic versus extra-synaptic NMDA receptors in our patches (Rosenmund et al., 1995). Before pulling outside-out patches we used a stimulus protocol that should predominately block synaptic receptors while leaving extra-synaptic receptors relatively unaffected. Following localized electrical stimulation (see Methods), outside-out patches were excised from the synaptically active regions of the dendrites. NMDA currents were then evoked using the fast application system, and the current amplitude was monitored over time to assess the amount of NMDA receptors blocked by MK-801. To speed the recovery from block, patches were depolarized every

second minute from –80 mV to +20 mV, and 3-4 glutamate pulses were applied for 500 ms. The proportion of current recovered from MK-801 block was used as an relative index of the amount of synaptic receptors in the patches. As control we used patches excised from proximal regions of the apical dendrite where there are few synapses, and therefore mostly extra-synaptic receptors, as well as patches from the distal part of the dendrite that had received no synaptic stimulation (data under these two conditions were pooled in **Figure 10C**).

Patches from distal segments of dendrites with evoked synaptic activity showed a greater than nine-fold increase in NMDA current over the 10 minute recording period (Fig. 8C) (in two cases current increased over 20 fold after 20 minutes). Control patches showed only an approximately two-fold increase for the same time course. Any significant movement of NMDA receptors between the extra-synaptic and the synaptic receptor pools during the time course of our experiments could cause an overestimation of the number of synaptic receptors in our patches (Tovar & Westbrook, unpublished observations). While such complications limit our ability to be quantitative, the data suggest that the majority of glutamate receptors in our patches were located at synaptic sites.

Discussion

Summary

We have characterized the amplitude, agonist affinity, kinetics and single channel properties of glutamate receptor-mediated currents, and compared these properties across a wide range of the apical dendrites of CA1 pyramidal neurons. The main finding is that the mean amplitude of the AMPA current at least doubles with distance from the soma. This distance-dependent increase in AMPA receptor current could be the result of an increased receptor number, receptor density or some modification of receptor properties. Modified subunit composition (Keinänen et al., 1990; Verdoorn et al., 1991; Mosbacher et al., 1994; Swanson et al. 1997; Dingledine et al., 1999, reviewed by Roche et al., 1994; Solderling et al. 1994; Smart 1997) or different phosphorylation states (Knapp et al. 1990; Greengard et al., 1991; Mammen et al., 1997; Hayashi et al., 1997; Banke et al., 2000) can change the kinetic properties, ionic permeability, agonist affinity, current-

voltage relationship, single-channel conductance and maximum open-probability of AMPA channels. We examined all of these receptor properties and compared them with distance from the soma, and found no significant differences in any of them, while on the other hand, channel number increased approximately two-fold. These data then strongly suggest that the distance dependent increase in AMPA current is due to a progressive increase in number of AMPAR in the patches and not to alterations in the basic properties of the receptor/channels.

Most of our results, AMPA receptor agonist-affinity, rise time, single-channel conductance and the concentration-dependency of AMPA and NMDA current kinetics, fit well with those previously published for similar experiments (Jonas & Sakmann, 1992; Spruston et al., 1995). There are, however, slight differences in deactivation and desensitization time constants for both receptor types (AMPA, NMDA). The kinetics reported here are slightly faster than those reported previously and this difference is likely to be due to developmental changes occurring in the receptors (our data being from adults and theirs from juveniles)(Jonas & Sakmann, 1992; Spruston et al., 1995). The calculated $P_{0,max}$ reported here is greater than that previously reported (Spruston et al., 1995) and this is surely the result of our use of a higher glutamate concentration (10 mM versus 1 mM) for the non-stationary fluctuation analysis experiments (see Silver et al., 1996). Finally, this is the first report of a distance-dependent increase in AMPA current amplitude and this too may be due to age differences or to the limited distance of the previous dendritic recordings (<175 μm) (Spruston et al., 1995).

Implications for distance-dependent synaptic scaling

These data fit well with the previous finding that the average conductance of Schaffer-collateral synapses increases some two-fold with distance from the soma and as expanded on below suggest that an increase in AMPA receptor numbers may be a primary mechanism of this increased conductance. The postsynaptic densities (PSD) of Schaffer collateral synapses show a wide range of sizes and the number of AMPA receptors present at these synapses increases directly with the PSD length (Takumi et al., 1999). Furthermore, spine head volume, PSD area and presynaptic terminal volume and active

zone (AZ) areas all vary together and show a wide range of sizes (Nusser et al., 1998; Schikorski & Stevens, 1999).

In light of these data, it seems possible that the average size of the Schaffer collateral synapses could increase with distance from the soma. In fact, similar changes have already been observed in other central neurons. The size and complexity of various pre- and postsynaptic components, including glycine receptor clusters, increases with distance from the soma of Mauthner cells (Triller et al., 1990, Sur et al., 1995). Furthermore, the size of gephyrin clusters, a protein involved in the clustering of glycine receptors, increases in size and complexity with distance from the soma of motoneuron and Ia inhibitory interneurons (Alvarez et al., 1997). Finally, spine head volume has been observed to increase significantly with distance from soma in the apical dendrites of mouse hippocampal and neocortical pyramidal neurons (Konur et al., unpublished observations). Thus, the distal regions of CA1 pyramidal neuron dendrites may possess a greater number of large area Schaffer collateral synapses that contain more AMPA receptors and we were able to observe this increase as larger amplitude AMPA currents.

AMPA and NMDA receptors are co-localized in at least 75% of Schaffer collateral synapses, (Takumi et al., 1999) and the ratio of receptor numbers changes as a linear function of PSD diameter. While the number of AMPA receptors showed a linear correlation to PSD area, the NMDA receptor numbers were independent of synapse size. Our patch data is consistent with these data in that the NMDA receptor number remains constant regardless of distance from soma. That NMDA receptor number remains constant while AMPAR numbers increase, suggest that the observed increase in AMPA receptor current is not due to any distance-dependent changes in patch area, spine density, or receptor access.

That we have observed distance-dependent changes in some of the postsynaptic properties of Schaffer collateral synapses does not exclude the possibility of other synaptic changes as well. In fact as the size of the axon terminal, AZ and number of docked vesicles all change together with postsynaptic properties it is likely that presynaptic modifications exist wherever there are postsynaptic changes. Furthermore, as with other synapses, Schaffer-collateral terminals are capable of releasing multiple quanta from multiple release sites (Bolshakov et al., 1997; Larkman et al., 1997; Prange

& Murphy, 1999; Bykhovskaia et al., 1999; Sorra & Harris, 1993). Theoretically, the occurrence of multi-synaptic boutons or the number of release site per bouton could also increase with distance from soma (Sur et al., 1995; Larkman et al., 1997). Any of these changes can cause an elevated synaptic conductance and given the covariance of many of these synaptic properties it seems likely that many changes together will be responsible for the increased conductance of distant synapses.

Mechanism of distance dependent scaling

For synapses to use a distance-dependent scaling to remove the location-dependence of synaptic efficacy requires these synapses to have some indication of their physical location in the dendritic arborization. This leads to the important questions; what signals are available to provide synapses with a distance-dependent cue and how might this signal be translated into changes in synaptic strength? To us it seems most likely that the distance-dependent regulation of AMPA receptor numbers and synaptic conductance are under the control of mechanisms similar to those described for homeostatic plasticity (Turrigiano & Nelson, 1998; Turrigiano et al., 2000). In homeostatic plasticity synaptic currents are scaled relative to postsynaptic activity, with action potential blockade leading to increases in EPSC amplitude, postsynaptic glutamate responsiveness, AMPAR half-life and AMPAR numbers. Along these lines, it is now well appreciated that the amplitudes of dendritic action potentials and the calcium influxes associated with them are dependent on distance from the soma, with both decreasing in amplitude with distance (Magee et al., 1998). Furthermore, there is some evidence that resting cytosolic [Ca] is reduced with distance from the soma (Magee et al., 1996). Together these observations lead us to propose that the reduced excitability of the distal dendrites alter the structure and composition of the synapses located there in a manner that increases their unitary conductance.

In conclusion, we have observed a distance-dependent increase in the amplitude of AMPA receptor-mediated currents in the apical dendrites of CA1 pyramidal neurons. The magnitude of this increase closely matches that observed for Schaffer collateral synapses across the same range of dendritic regions. In the light of this observation and because no differences in a variety of AMPA channel properties were observed, we

conclude that an increase in the amount of AMPA receptors elevates the conductance of distant Schaffer collateral synapses in hippocampal CA1 pyramidal neurons.

Part II.

Impaired regulation of synaptic strength in hippocampal neurons from GluR1-deficient mice

Neurons of the central nervous system (CNS) exhibit a variety of forms of synaptic plasticity; including associative long-term potentiation and depression (LTP/D); homeostatic activity-dependent scaling and distance-dependent scaling. A regulation of synaptic neurotransmitter receptors is currently thought to be a common mechanism among many of these forms of plasticity. In fact, glutamate receptor 1 (GluR1 or GluRA) subunit containing L-α-amino-3-hydroxy-5-methylisoxazle-4-propionate (AMPA) receptors have been shown to be required for several forms of hippocampal LTP and a particular hippocampal-dependent learning task. Because of this importance in associative plasticity, we sought to examine the role of these receptors in other forms of synaptic plasticity in the hippocampus. Virtually all CNS neurons involved in fast glutamatergic synaptic transmission express AMPA receptors and the great diversity of biophysical properties provided by these receptors makes them highly suitable for meeting many distinct physiological requirements (Wenthold et al., 1996, Geiger et al., 1997, Trussel, 1999). This variety of functional capabilities stems from the fact that most native AMPA receptors are composed of at least two different subunits (out of four GluR1-4 gene products) that form a penta- or tetrameric receptor-channel complex (reviewed in Dingledine et al., 1999). In addition, alternative splicing and RNA editing of receptor subunits adds to the diversity of receptor-channel compositions. Accordingly, specific expression patterns exist throughout the CNS with groups of neurons preferentially expressing one or two of the AMPA receptor subunits. For example, a prevalence of GluR4 has been found at fast auditory synapses (Trussel, 1999) while primarily GluR1 expressing neurons have been identified in cortex, striatum and spinal cord (Petralia and Wenthold, 1992; Furuyama et al., 1993; Martin et al., 1993; Tachibana et al., 1994). Hippocampal CA1 pyramidal neurons produce multiple AMPA receptor complexes that

are comprised of mainly GluR1 or GluR2 containing AMPA receptors (Wenthold et al., 1996).

GluR1 containing AMPA receptors are thought to be intimately involved in the regulation of synaptic strength in many neurons including CA1 neurons. Their ability to increase synaptic strength through either an activity-dependent delivery of new receptors (Hayashi et al., 2000; Shi et al., 2001; Passafaro et al., 2001; Lu et al., 2001; Piccini & Malinow, 2002) or an increase in single channel conductance (Benke et al., 1998; Derbach et al., 1999) has been well documented in several associative forms of synaptic plasticity. It is also possible that, a regulated synaptic delivery of AMPA receptors may be involved in modulations of synaptic strength occurring over longer time-scales, such as homeostatic activity- and distance-dependent synaptic scaling (Inasek & Redman, 1973; Korn et al., 1993; Turrigiano et al., 1998; van Rossum et al., 2000; Turrigiano & Nelson, 2000; Burrone et al., 2002; Andrásfalvy & Magee, 2001; Smith et al., 2003). These separate forms of plasticity adjust overall synaptic strength to maintain a particular degree of synaptic influence over ongoing neuronal activity for any given level of postsynaptic excitability or synapse location (Turrigiano & Nelson, 2000; Magee, 2000). The role of GluR1 containing AMPA receptors in such longer time-scale modulations of synaptic strength has, however, not been previously investigated.

In light of this, we have examined the impact of GluR1 deletion on the dendritic pools of AMPA receptors using a wide variety of recording techniques in hippocampal CA1 pyramidal neurons. Data presented here indicate that 1) the extra-synaptic pool of AMPA receptors is almost exclusively composed of GluR1-containing receptors, 2) the synaptic pool of AMPA receptors also contains a large contingent of GluR1-containing receptors, 3) a location-dependent insertion of GluR1-containing AMPA receptors produces distance-dependent scaling of Schaffer collateral synaptic strength in CA1 pyramidal neurons. Together these data further demonstrate the fundamental role that the cycling of GluR1 containing AMPA receptors plays in regulating synaptic strength in these neurons.

Results

AMPA current in dendritic outside-out patches

We began by assessing the impact of GluR1 subunit deletion on the dendritic AMPA receptor population. To do so we compared currents produced by the rapid application of glutamate to outside-out patches excised from different dendritic regions of hippocampal CA1 pyramidal neurons from both wild type (WT) and GluR1 -/- (KO) mice (**Figure 11A-D**). The AMPA component of patches excised from a location where there are essentially no excitatory synapses (~20 μm from the soma) was decreased by approximately 97 % in GluR1 -/- mice (WT: 541 ± 108 pA, n = 9; KO: 11 ± 2 pA, n = 9; $p < 0.001$, **Figure 11E**). A similar magnitude of reduction was also detected at a more distal region (170-200 μm) where spine and synaptic density is high (WT: 874 ± 136 pA, n = 8; KO: 25 ± 8 pA, n = 12; $p < 0.001$, **Figure 11E**).

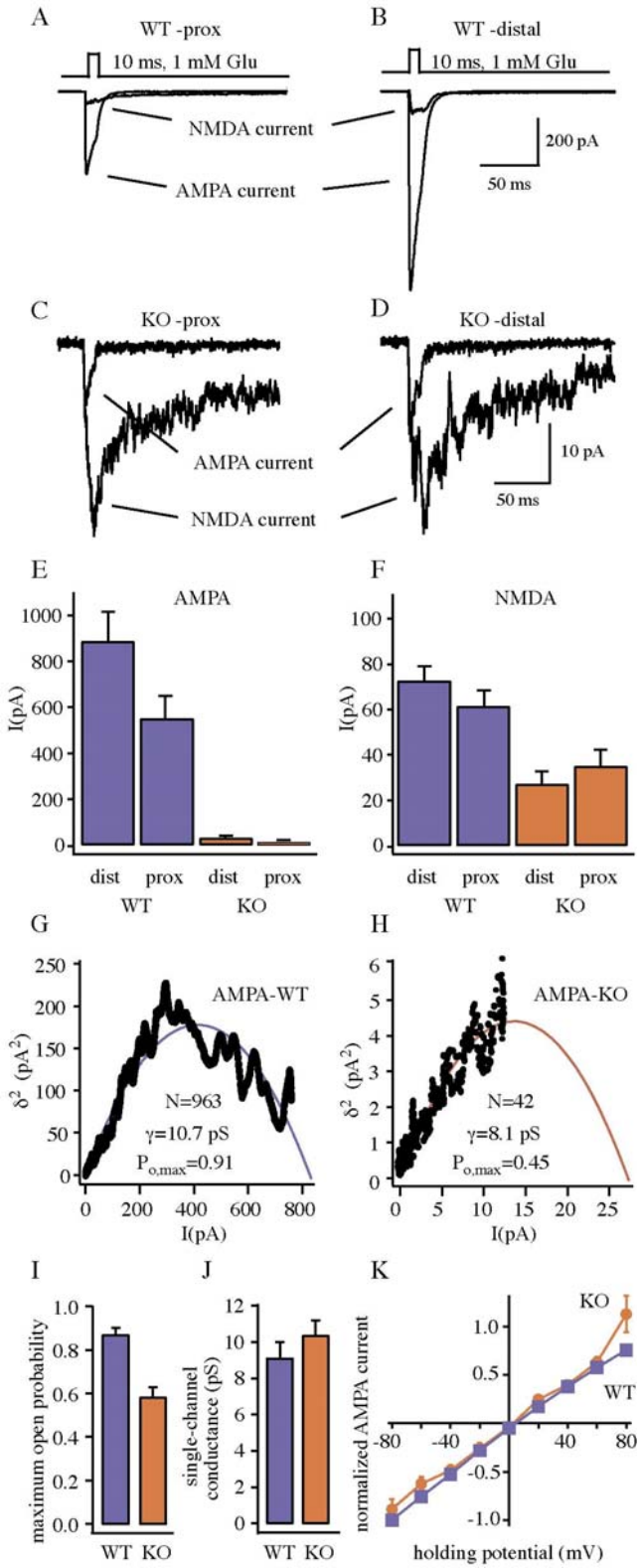

Figure 11. The extra-synaptic pool of AMPA and NMDA receptors is severely altered in GluR1 -/- mice. Representative AMPA and NMDA receptor current traces, evoked by rapid glutamate applications to dendritic outside-out patches, are shown for proximal (A, **C**) and distal patches (**B, D**) from wild type (**A, B**) and GluR1 -/- mice (**C, D**). Currents are the averages of 3-5 individual traces. Mean AMPA (**E**) and NMDA (**F**) receptor current amplitudes are shown for all groups; where blue bars are WT and red bars are KO mice. Representative non-stationary fluctuation analysis (NSFA) of distal patches from WT (**G**) and KO (**H**) mice. Note that patches from KO mice have a dramatic reduction in receptor number (**N**), and maximum open-probability ($P_{o,max}$) (**I**), while the single-channel conductance (γ) is the same in both groups (**J**). **K**, Current-voltage relationships of AMPA receptor currents are similar between WT (blue) and KO (red) mice. WT: E_{rev} = 5.0 ± 0.5 mV, n = 11; KO: E_{rev} = 2.0 ± 1.0 mV, n = 4.

That AMPA receptor currents from both spiny and non-spiny regions were reduced by comparable magnitudes strongly suggests the receptors in outside-out patches are from extra-synaptic regions despite of our previous postulation (Andrásfalvy and Magee, 2001) and that this pool is almost completely devoid of AMPA receptors in GluR1 -/- mice. Interestingly, the NMDA receptor component from GluR1 -/- mice was likewise reduced in both regions by approximately 50%, implying a linkage between AMPA and NMDA receptor numbers in extrasynaptic receptor pool (**Figure 11F**).

Channel subunit composition

Channel subunit composition has been shown to play a determining role in many of the basic properties of various agonist-gated ion channels, including AMPA receptors (Verddon et al., 1991; Mosbacher et al., 1994; Swanson et al., 1997). Therefore to examine this more closely we compared the AMPA receptor current kinetics, voltage dependence and single channel properties in patches from WT and KO mice. From these patches we saw that current rise time constants were not altered, while AMPA receptor deactivation time constants and the fast component of desensitization were significantly faster in GluR1 -/- mice (**Figure 12**). Also the fast component of desensitization was much more prominent in patches from KO mice (**Figure 12A-E**). Furthermore, non-stationary fluctuation analyses indicated that the calculated maximum open-probability ($P_{o,max}$) was heavily reduced in KO mice while single-channel conductance (γ) was identical in WT and KO mice from both locations (**Figure 11G,H**). Finally, current-voltage relationships were very similar in both sets of mice except for a slight shift in reversal potential (WT: E_{rev} = 5.0 ± 0.5 mV, n = 11; KO: E_{rev} = 2.0 ± 1.0 mV, n = 4; $p < 0.001$ **Figure 11K**). All of the above AMPA receptor properties were independent of patch location.

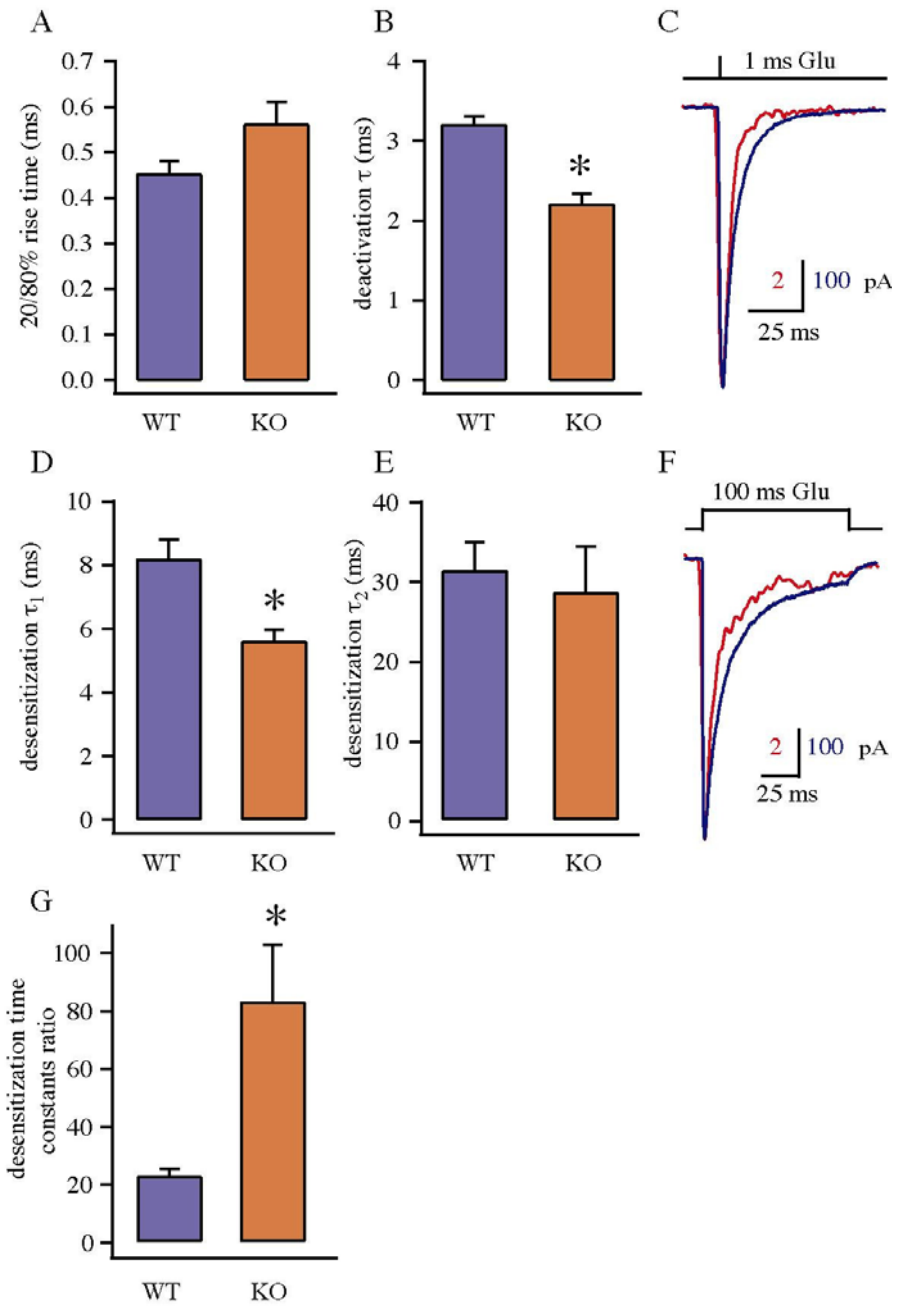

Figure 12. Some kinetic properties of AMPA currents are altered in GluR1 -/- mice. **A**) Rise times of outside-out patch currents are not altered (WT, blue: 457 ± 34 µs, n = 16; KO, red: 568 ± 50 µs, n = 8; p >0.05), while **B**) the deactivation time constants (WT: 3.2 ± 0.2 ms, n = 8; KO: 2.2 ± 0.2 ms, n = 12, p <0.001) and **D**) the fast component of desensitization (WT: 8.1 ± 0.7 ms, n= 8; KO: 5.6 ± 0.4 ms n = 12, p <0.05) are significantly faster in GluR1 -/- mice. **G**) Also the fast component of desensitization is much more prominent KO mice (WT: desen. ratio 22 ± 2 %, KO desen. ratio 82 ± 20 %, p <0.001). Representative AMPA receptor currents, evoked by 1 (**C**) and 100 ms (**F**) glutamate pulses (1 mM), are shown for WT (blue) and KO (red) dendritic patches.

The observation that both γ and the current-voltage relationships of WT and GluR1 -/- mice were similar indicates that the GluR2 containing heteromeric (GluR1/2 and/or GluR2/3) subunit composition is dominant in both groups of mice (Verddon et al, 1991; Mosbacher et al, 1994; Swanson et al, 1997). Otherwise, γ should have dramatically decreased if homomeric GluR2 receptors were formed and, a major rectification change would have been seen in the case of homomeric GluR3 or $GluR2_{long}$ and heteromeric $GluR2_{long}$/3 receptors (Verddon et al, 1991; Mosbacher et al, 1994; Swanson et al, 1997; A. Kolleker et al., unpublished observation). Thus it is most likely that under control conditions the vast majority of the receptors in the extra-synaptic pool are GluR1/2 heteromers with GluR2/3 heteromers providing only a small component of receptors that appear to have a significantly reduced $P_{o,max}$ or glutamate affinity and faster channel kinetics.

Synaptic currents and distance-dependent scaling.

As mentioned above, the cycling of AMPA receptors between extra-synaptic and synaptic pools is thought to be a critical component in many forms of synaptic plasticity (Zamanillo et al., 1999; Lu et al, 2001; Piccini and Malinow, 2002; Andrásfalvy and Magee, 2002). The nearly complete loss of the extra-synaptic pool of AMPA receptors in the GluR1 -/- mice strongly suggests that this receptor cycling should be essentially absent in CA1 pyramidal neurons from these mice. We, therefore, tested the idea that cycling plays a fundamental role in establishing distance-dependent scaling by comparing the location-dependence of synaptic currents in CA1 neurons from both WT and KO mice. Whole-cell recordings from different regions of the apical dendritic arbor were used to record miniature excitatory postsynaptic currents (mEPSCs), evoked by the localized application of a high osmolarity external solution (see methods, **Figure 13A,B**) (Magee and Cook, 2000; Smith et al. 2003). Consistent with data obtained from rats (Magee and Cook, 2000; Smith et al. 2003), distal mEPSC amplitudes in WT mice were approximately two-fold larger than proximal events (prox.: 11.7 ± 0.9 pA, n = 5, vs distal: 24.2 ± 2.3 pA, n = 6, **Figure 13C,E**). GluR-1 -/- mice, on the other hand, exhibited a greatly reduced distance-dependent scaling of synaptic amplitude (prox: 8.2 ± 0.8 pA, n = 6, distal: 10.1 ±

0.9 pA, n = 8, p >0.05; **Figure 13D,F**), as compared to wild type mice (WT: 107 % increase vs KO: 23 % increase). Also, mEPSC rise time constants in GluR1 -/- mice were found to be slightly faster than in WT mice while no differences were detected in mEPSC decay time constants (**Figure 13I,J**). The mEPSC data show that GluR1 containing AMPA receptors are a significant component of the synaptic pool of AMPA receptors at Schaffer collateral (SC) synapses and furthermore that GluR1 receptors are required for distance-dependent scaling in CA1 pyramidal neurons. The loss of this compensatory modulation of synaptic strength causes a location-dependent reduction in basal synaptic strength in GluR1 -/- mice with proximal synapses experiencing much less attenuation than more distal synapses. Thus, as discussed below, it is possible that a location-dependent difference in the proportion of GluR1 containing AMPA receptors exists at SC synapses under normal conditions.

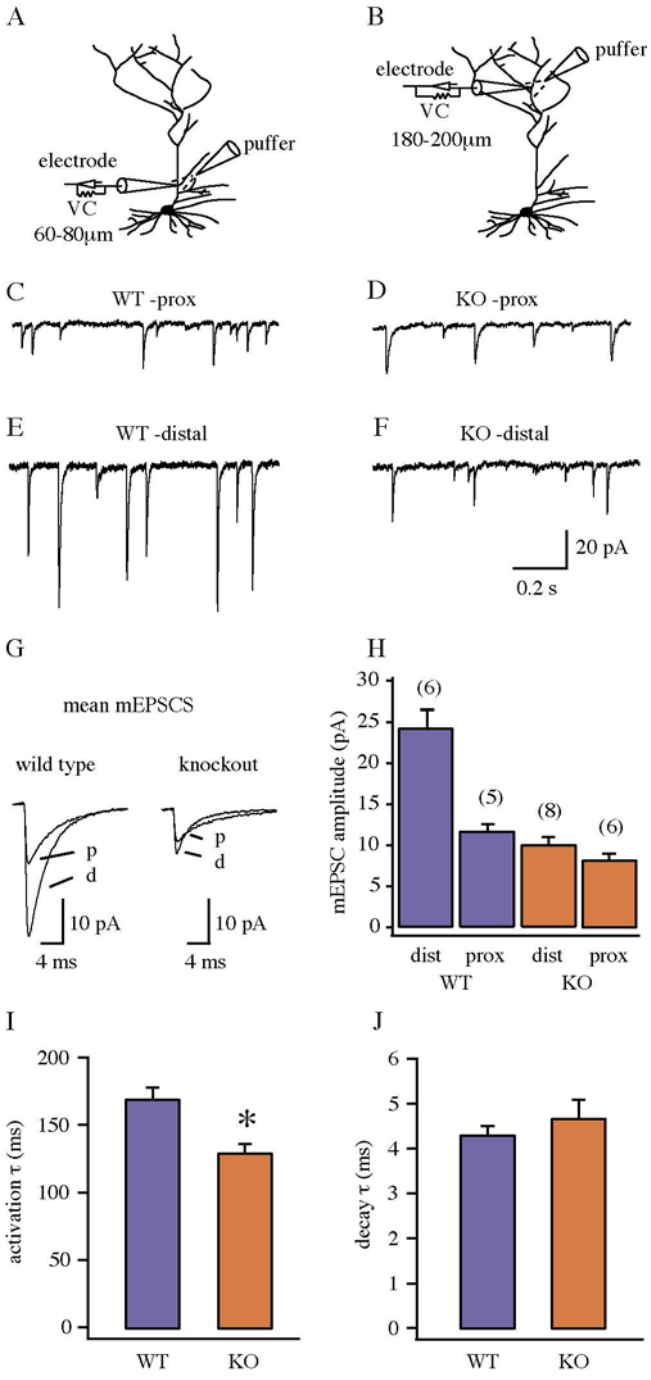

Figure 13. Distance-dependent scaling of synaptic current amplitude is attenuated in GluR1 -/- mice. **A**) Schematic diagrams of proximal and **B**) distal dendritic voltage-clamp recording configurations. **C-F)** Representative recordings of hypertonically-evoked synaptic activity from proximal and distal dendrites in wild type and in GluR1 -/- mice, respectively. **G**) Averages

of 100-165 individual mEPSCs from each of the recordings shown above. p and d represent proximal and distal recordings respectively. **H**) Grouped data of mean mEPSC amplitude for all cells. Numbers of cells are shown above each bar. **I**) mEPSC rise time constants in GluR1 -/- mice are slightly faster than in WT mice, and this increase is independent of synaptic location (WT: 175 ± 9 μs, n = 11; KO: 134 ± 7 μs, n = 14, p <0.001). J, No differences are detected in mEPSC decay time constants (WT: 4.3 ± 0.2 ms, n = 11; KO: 4.7 ± 0.4 ms, n = 14).

GluR1 and quantal size

To determine the mechanism by which GluR1-containing AMPA receptors modulate the basic synaptic weight of SC synapses we performed additional analyses of the synaptic currents. Further examination of the current data revealed that the distribution of mEPSC amplitudes were highly variable in all groups (CV >50 %, **Figure 14A**). While no differences in the coefficients of variation were observed for either synapse location or mouse type, a large location-dependence was observed for the parameter σ^2/x in only the WT mice (**Figure 14B**). These data suggest that there is an increase in the quantal size at distal WT synapses that does not occur in GluR1 -/- mice. Furthermore, the large amount of positive skew (skewness: 1.2 ± 0.03) observed in the amplitude distributions suggests that they might be composed of multiple components (**Figure 14G**). In fact the distributions from most neurons were well fit by multiple Gaussian functions, with peak separation increasing with distance, again, in only the WT mice (see methods, **Figure 14C-G**). Finally, cumulative frequency distributions demonstrate that distal synaptic inputs from WT mice are uniformly shifted towards larger amplitudes, while proximal WT and both proximal and distal distributions from KO mice almost overlap at lesser amplitudes (**Figure 14H**). Together these statistical data suggest that the amplitude of distal mEPSCs are increased in WT mice by a scaling-up of either postsynaptic AMPA receptor effectiveness or the amount of glutamate packaged into a synaptic vesicle. That this scaling is not found at distal synapses of GluR1 -/- mice points strongly towards an effect mediated though postsynaptic receptors and not presynaptic vesicular content, also the lack of any significant differences in pair-pulse facilitation ratios among the groups further support this interpretation (**Figure 14I**) and (Zamanillo et al, 1999). The evidence thus far presented points towards the idea that a location dependent delivery of GluR1

containing AMPA receptors increases the quantal size of distal SC synapses, resulting in a distance-dependent scaling of synaptic weight.

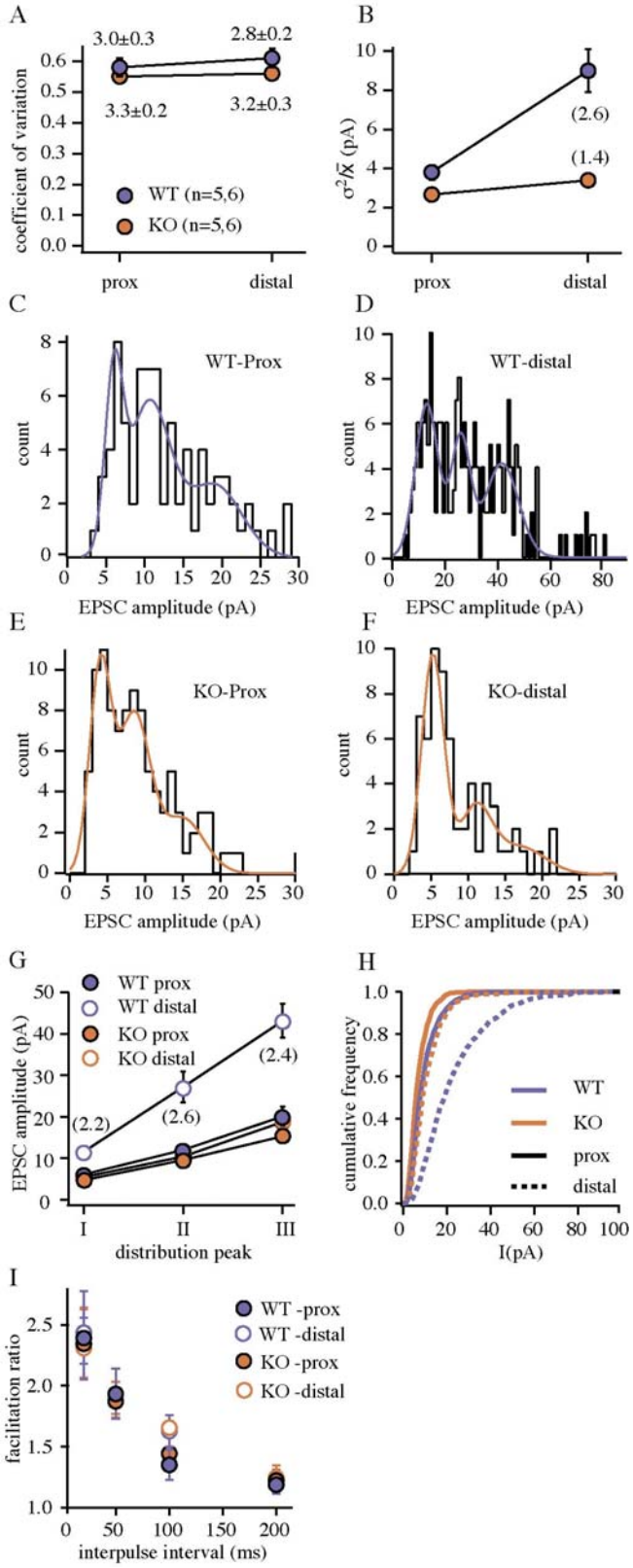

Figure 14. Synaptic current distributions from GluR1 -/- mice show altered properties. **A**) Plot of CV for all four groups of mEPSCs. Numbers shown on plot are mean $1/cv^2$, a measure that is indicative of quantal content. **B**) Plot of σ^2/x for the four groups of mEPSCs. This measure is indicative of quantal size and the plots indicate that the normal distance-dependent increase in this parameter is absent in GluR1 -/- mice. Amount of increase in σ^2/x from proximal locations to distal (distal/prox) are displayed on the plot. **C-F**) mEPSC amplitude distributions of proximal (prox) and distal synapses from wild type (WT) and knockout mice (KO). Between 135 and 204 events were plotted using a bin size of 1 pA. Solid lines are fits of data by the sum of three Gaussians with individual mean peaks at WT-prox x1 = 6, x2 = 10, x3 = 20 pA; WT-distal x1 = 13, x2 = 25, x3 = 42 pA; KO-prox x1 = 4, x2 = 8, x3 = 15 pA; KO-distal x1 = 6, x2 = 12, x3 = 17 pA. **G**) Plot of mean peak amplitudes from the multiple Gaussian fits for each group of distributions. Numbers on plot are the ratio of WT distal to all other group peak amplitudes, suggesting again that distal synapses in GluR1 -/- mice lack an approximately 2.5 fold increase in quantal size. **H**) Cumulative frequency distribution of all events from WT (blue) and GluR1 -/- (red) mice. Solid lines are proximal and dashed lines are distal distributions. **I**) Pair-pulse facilitation ratios ($EPSC_{2nd}/EPSC_{1st}$) are shown at four

different inter-stimulus intervals, recorded and stimulated at proximal (filled circle) and distal (open circle) dendritic regions, from WT (blue) and KO (red) mice.

Synaptic AMPA receptor currents

To further examine the possible mechanisms of the loss of distance-dependent scaling in KO mice, the location-dependence of synaptic AMPA receptor currents was determined by focally applying glutamate onto isolated dendritic spines using multi-photon un-caging of MNI-glutamate (Matsuzaki et al., 2001; Smith et al, 2003). Glutamate was released near well-isolated spines either on the dendritic trunk or radial oblique dendrites that were within 20 μm of the dendritic recording pipette (**Figure 15A-D**). In wild type mice, the mean AMPA receptor mediated current obtained from proximal spines was 32 ± 4 pA (16 spines from 7 cells; spine volume: 0.11 ± 0.01 μm^3) compared with 69 ± 4 pA at distal spines (13 spines from 6 cells; spine volume: 0.10 ± 0.01 μm^3) (**Figure 15F**). Therefore, as previously observed in rats, distal spines from wild type mice show a nearly two-fold increase in AMPA receptor mediated glutamate responsiveness when compared to proximal spines (Smith et al., 2003). However this large distance-dependent increase in AMPA receptor current was not observed in the spines of KO mice ($p > 0.05$), such that proximal amplitudes were 26 ± 3 pA (13 spines from 6 cells; spine volume: 0.10 ± 0.01 □m^3) and distal amplitudes were 33 ± 2 pA (14 spines from 6 cells; spine volume: 0.11 ± 0.01 □m^3; **Figure 15F**). In all groups, the glutamate currents had similar rise and decay time constants (see **Figure 15G,H**).

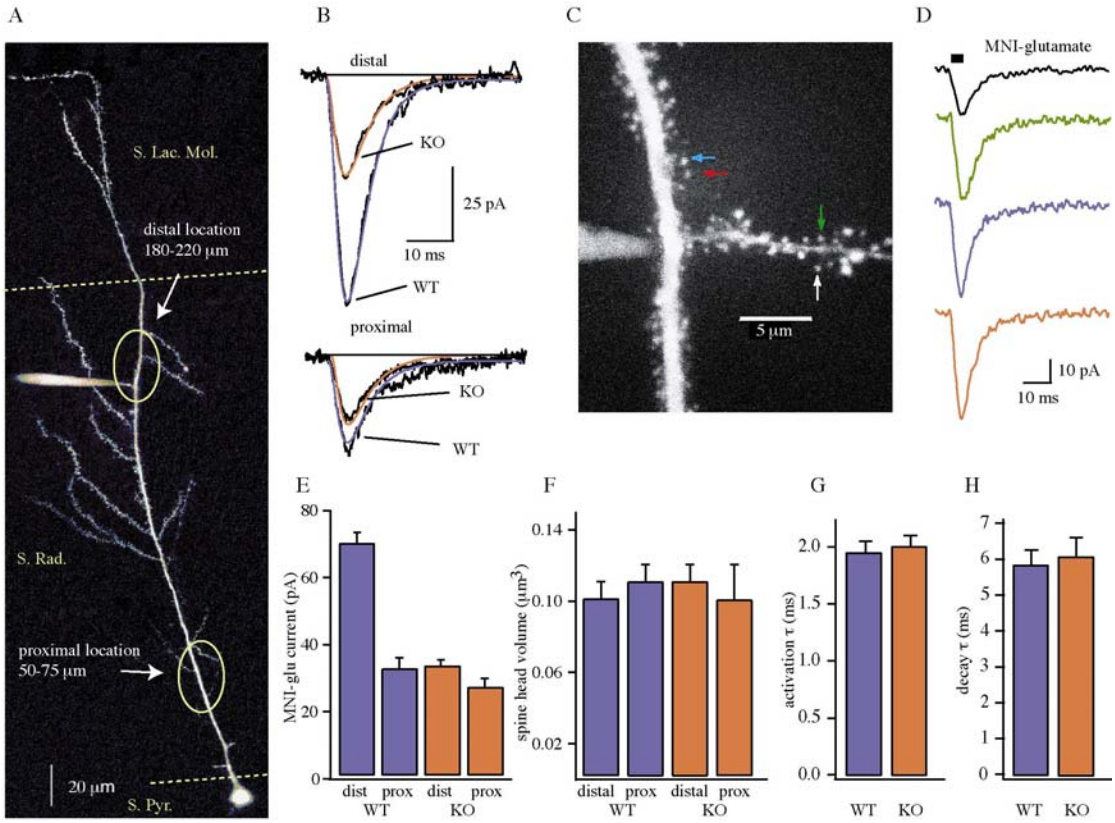

Figure 15. The synaptic pool of AMPA receptors is reduced in a location-dependent manner in GluR1 -/- mice. **A**) Image stack spanning the entire apical dendritic arborization of another CA1 pyramidal neuron. Ovals represent distal and proximal recording sites in stratum radiatum (S. Rad). Dashed lines demonstrate the proximal stratum pyramidale (S. Pyr.) and the distal stratum lacunosum-moleculare (S. Lac. Mol.) borders of stratum radiatum. **B**) Location dependent AMPA currents from WT and KO mice, averages of 2-3 traces. Traces are fit by the sum of two exponential with blue lines for WT and red for KO mice. Note that the distant-dependent increase in AMPA current is missing in the records from the KO mice. **C**) Multi-photon image stack of a distal dendritic region of a CA1 pyramidal neuron filled with bis-fura2. The dendritic recording electrode is shown at left and the colored arrows indicate the isolated spines that gave the correspondingly colored MNI-glu currents shown to the right. **D**) Examples of AMPA receptor currents evoked by focal un-caging of MNI-glutamate (MNI-glu) onto isolated spines located on the main dendritic trunk and a nearby oblique dendrite (branch to the right), as indicated by colored arrows shown in **C, E**) Mean AMPA current amplitudes for wild type (blue bars) and GluR1 -/- (red bars) mice. **F**) The spine head volume were the same in both group of mice in both location. **G,H**) In all groups of MNI-glu currents have similar time constants of rise (WT: 1.95 ± 0.1 ms, n = 29; KO: 2.0 ± 0.1 ms, n = 23) and decay (WT: 5.85 ± 0.4 ms, n = 29; KO: 6.1 ± 0.5 ms, n = 23).

Therefore, the distance-dependent increase in postsynaptic AMPA receptor current that is normally found in these neurons is absent in the GluR1 -/- mice, just as was observed above for the spontaneous synaptic currents. The observed reduction in the spine AMPA current in KO mice is comparable to that seen in mEPSC amplitude and is much less than that observed in the dendritic patches, thus lending credence to the idea that most of the AMPA receptors activated by glutamate un-caging are synaptic in origin while those in the patches are from extra-synaptic sources (**Figure 16A,B**). These data strengthen the idea that distal Schaffer collateral synapses normally contain a higher density of AMPA receptors that increase the responsiveness of the synapse to quantal glutamate release and furthermore that this increase is dependent upon the presence of GluR1-containing AMPA receptors.

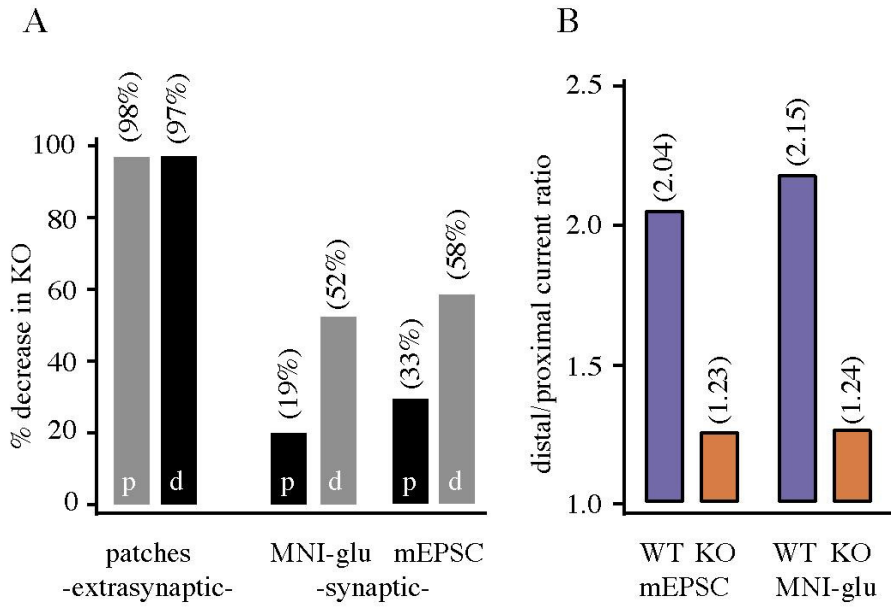

Figure 16. Almost empty extrasynaptic AMPA receptor pool and reduced synaptic pool in a location-dependent manner in GluR1 -/- mice. **A**) Decrease in amplitude observed in GluR1 -/- mice for AMPA currents recorded in outside-out patches (patches), glutamate un-caging (MNI-glu) and mEPSCs (mEPSCs). Note that mEPSC and MNI-glu currents are similarly reduced while patch currents are reduced to a much greater extent. p is proximal currents and d is distal currents. **B**) Plot of the increase in distal current amplitude for mEPSCs and MNI-glu currents in both wild type and GluR1 -/- mice. Notice the increases in mEPSCs amplitudes are mirrored by the increases in MNI-glu current.

Discussion

Summary

We have characterized the properties of dendritic AMPA receptors, spontaneous synaptic currents and postsynaptic AMPA receptor responsiveness in hippocampal CA1 pyramidal neurons from both wild type and GluR1 -/- mice. The main observations are; **1**) AMPA receptor currents from outside-out patches pulled from the apical dendrites of GluR1 -/- mice are severely reduced in amplitude. **2**) These currents from the KO mice also appear to decay faster and have a lower probability of opening than WT currents. **3**) Spontaneous synaptic currents are also smaller in amplitude in the KO mice and the degree of this reduction is dependent on the dendritic location of the synapse, with distal synapses showing the greatest reduction. **4**) Statistical analyses of the synaptic currents indicate that the distal SC synapses of KO mice lack a normal increase in postsynaptic responsiveness, and focal application of glutamate onto postsynaptic spines confirms this scenario. We interpret these data to indicate that the extra-synaptic pool of AMPA receptors is almost entirely composed of GluR1-containing AMPA receptors (probably GluR1/2 heteromeres) and that distance-dependent scaling of SC synaptic weight is the result of an increased delivery of these receptors to distal synapses. Furthermore, this regulated delivery probably involves receptor cycling between the synaptic and extra-synaptic pools of AMPA receptors.

Increased density of GluR1 at distal synapses

The similarities in the ratios of distal to proximal mEPSCs and postsynaptic AMPA receptor currents in both WT and KO mice (**Figure 16B**), as well as the lack of any significant differences in pair-pulse facilitation ratios (**Figure 14I**) and (Zamanillo et al., 1999), all minimize the likelihood that an alteration in presynaptic vesicular release is responsible for the loss of synaptic scaling in GluR1 -/- mice. Instead, the spine-level differences in AMPA receptor currents, revealed by multi-photon glutamate un-caging, suggest that distal synapses of WT mice have either greater numbers or more effective AMPA receptors. We suspect that the number of AMPA receptors is elevated at distant synapses because we have observed such an increase in rat hippocampal CA1 pyramidal neurons (Smith et al., 2003). Accordingly the impaired glutamate responsiveness observed

in GluR1 -/- mice seems to indicate that a deficiency in the location-dependent insertion of AMPA receptors causes distance-dependent scaling of basal synaptic weight to be impaired in these mice. Having said this, it is possible that the differences in $P_{o,max}$ observed in the outside-out patch currents could also produce location-dependent synaptic currents if there were differences in the proportion of the higher $P_{o,max}$ GluR-1-containing heteromeres present at the synapses. In this case if distal synapses contain relatively more GluR1-containing AMPA receptors compared to more proximal synapses the higher $P_{o,max}$ of those AMPA receptors could add additional weight to the distal synapses. Given the data from rat CA1 cells, however, we find it more likely that the main mechanism of synaptic scaling is an increased delivery of GluR1-containing AMPA receptors that in turn might also have a higher $P_{o,max}$.

AMPA receptor cycling and homeostatic synaptic plasticity

Previous studies have demonstrated subunit-specific AMPA receptor transportation routes where GluR2/3 receptors are delivered by direct insertion and continuous recycling within the synapse. Modulations of this cycling are thought to set basal synaptic strength and underlie some forms of LTD (Shi et al., 2001; Kim et al., 2001). GluR1/2 receptors, on the other hand, are thought to initially insert into the extra-synaptic membrane and then move laterally into the postsynaptic density depending on the activity pattern of the synapse (Lu et al., 2001; Piccini & Malinow, 2002; Andrásfalvy & Magee, 2002). This scheme is supported by observations that GluR1 -/- mice lack both a significant extra-synaptic AMPA receptor pool as well as most forms of associative LTP Zamanillo et al., 1999; Mack et al., 2001; Hoffman et al., 2002). That these mice also lack distance-dependent scaling suggests that longer time-scale modulations of synaptic strength also use the same GluR1 containing AMPA receptor delivery system to regulate basal Schaffer collateral strength.

Although both of these diverse forms of plasticity appear to use the same receptor delivery system, the induction rules governing the location-dependent addition of GluR1/2 receptors would not be the same as those seen in most forms of associative synaptic plasticity (where brief positive associations produce increased strength). Instead, there must be some variation of the standard activity-dependent induction rules that is perhaps

based on the differences in time-scale (where positive associations over many hours produce decreased strength, *personal communication, Larry Abbott*). Although the exact control mechanisms are still murky, it is clear that the highly regulated cycling of GluR1 containing AMPA receptors is fundamental to the modulation of synaptic strength in CA1 pyramidal neurons and, furthermore, that this modulation is critical for proper hippocampal functioning (Reisel et al., 2002).

Part III.
Changes in AMPA Receptor Currents Following LTP Induction on CA1 Pyramidal Neurons

The most extensively studied form of activity-dependent synaptic plasticity is long-term potentiation (LTP) of glutamatergic synapses in CA1 pyramidal neurons of the hippocampus. One model of this process holds that an influx of Ca^{2+}, mainly through NMDA receptors, initiates multiple mechanisms that result in an increase in transmission through AMPA type glutamatergic receptors (Bliss & Collingridge, 1993). A postsynaptic mechanism thought to play an important role in this form of synaptic plasticity is the enhancement of AMPA receptor function through some type of receptor/channel modification (Malinow et al., 2000). There are several different modifications of AMPA receptors that might result in an increased synaptic efficacy and these include; insertion of more receptors into the synaptic membrane (Malinow et al., 2000; Lu et al., 2001), increased channel open probability, increased single-channel conductance (Benke et al., 1998; Derkach et al., 1999), increased glutamate affinity or different channel kinetic properties.

There is evidence supporting an activity-dependent delivery of new, particularly GluR1-containing, AMPA receptors in various forms of long-term synaptic plasticity. Different types of immunocytochemical, over-expression approaches have suggested that an increased synaptic AMPA channel density follows the induction of a synaptic potentiation (Dudek & Bear, 1993; O'Brien et al., 1998; Heynen et al., 2000; Hayashi et al., 2000; Lu et al., 2001; Passafaro et al., 2001; Piccini & Malinow, 2002). There are still some questions, particularly in adult animals, however, revolving around whether most

receptors are directly inserted into the postsynaptic density (PSD) or diffuse laterally into the synapse from an extra-synaptic compartment. Furthermore there is other evidence, although primarily in young animals and expression systems, that changes in AMPA channel phosphorylation state can increase single channel conductance (Benke et al., 1998; Poncer et al., 2002).

We investigated the changes in AMPA receptor function that accompany LTP by comparing the properties of AMPA receptors in outside-out patches pulled directly from synaptically-active dendritic regions both in control conditions and following the induction of LTP and an experimentally-induced increase in intracellular CaMK-II activity. The data suggest that, in the adult rats used here, an increase in channel number and not a CaMK-II-dependent change in channel properties is the primary mechanism of the postsynaptic changes in synaptic efficacy found following the induction of LTP. Furthermore, we have found that this increase does not occur throughout the activated neuron and is dependent upon the presence of active spines.

Results

Measuring synaptic efficacy using cell-attached patch recordings

So as to not disturb the local intracellular environment, we monitored the electrical activity with a cell-attached patch recording for 10-20 min before and 20-30 min after tetanus stimulation (Frick et al., 2004). Every 20 seconds we gave 3 test stimuli (100 Hz), that were large enough to evoke one or two action potentials (AP). The recorded capacitive currents were analyzed by two separate criteria to evaluate the change in synaptic efficacy. First, we measured the first spike latency from the beginning of the recorded trace, based on the notion that the increased synaptic efficacy increases the depolarization of the neuron, so it reaches the threshold earlier in time (**Figure 17**). Second, we used the capacitive current traces as a measure of the evoked excitatory-post-synaptic-potantial (EPSP). The underlying idea is that during the potentiation the evoked EPSP increased and the elevated rate of voltage change (dV/dt) causes an elevated capacitive current ($I_c=C_m$ * dV/dt, where C_m is patch capacitance). Indeed following potentiation the deflection increased after tetanus (274 ± 48%; n=11, **Figure 17**), while

the deflection remained unchanged if the potentiation failed or was intentionally blocked by NMDA channel inhibition 110 ± 6%; n=12, **Figure 17**).

Dendritic region receiving stimulation

Although it is impossible to be exact, we can coarsely estimate the region of the dendrite being stimulated by the large amplitude electrical stimulation based on the following assumptions: we stimulated an approximately 20 μm^3 volume of radiatum, 30 μm away from the dendrite and SC axons innervating a particular dendrite can approach it from as much as a 45° angle (Sorra & Harris, 1993). Given these estimates and the complicated branching pattern of CA1 dendrites it is possible that up to a 100 μm length of the apical dendrite would receive tetanized synaptic input during the large amplitude electrical stimulation. These values fit well with previous observations of subthreshold dendritic Ca^{2+} influx associated with electrical synaptic stimulation (Magee et al 1995; Magee & Johnston 1997).

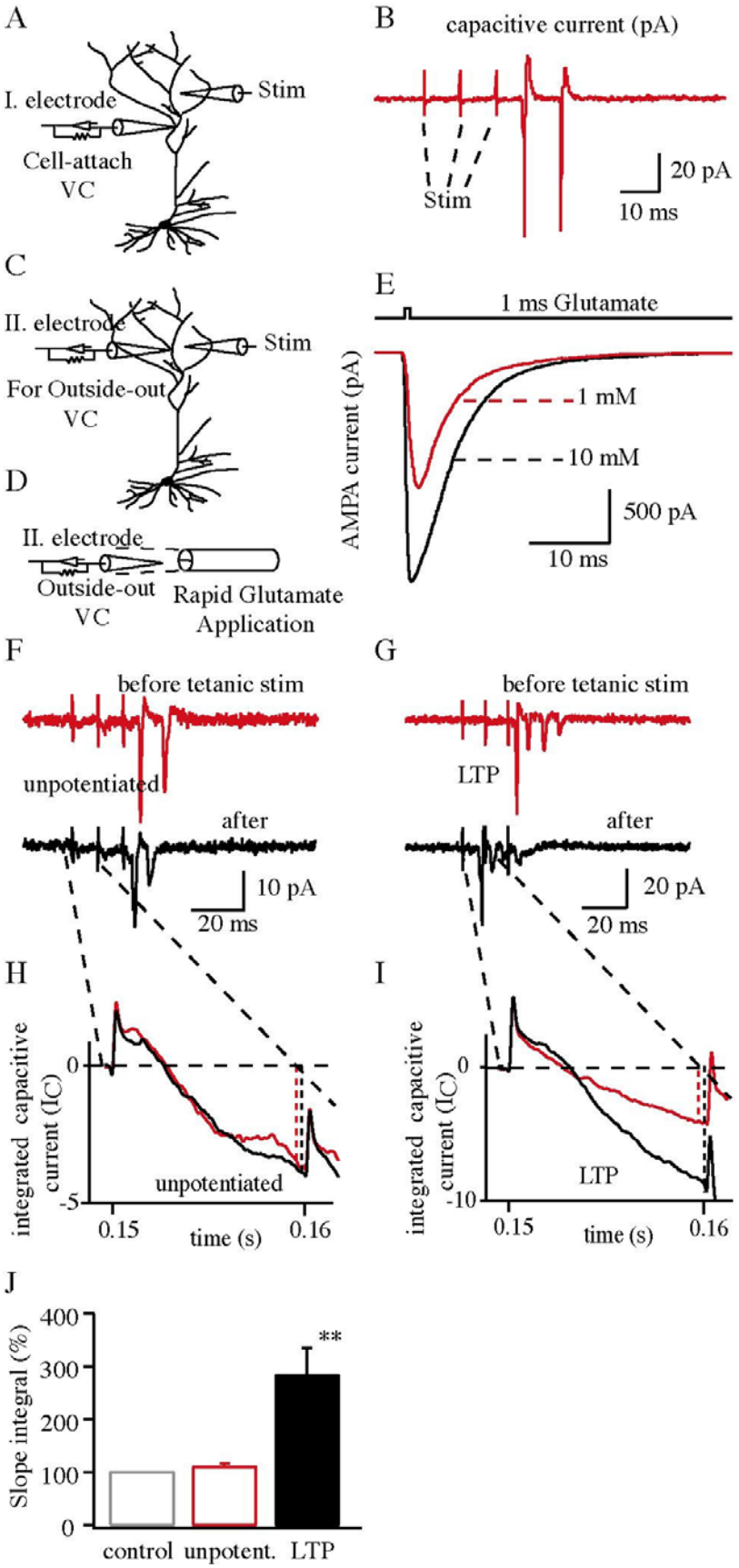

Figure 17. A) diagram of a dendritic cell-attached patch recording from ~150 µm distal from the soma. **B**) Representative trace of capacitive currents evoked by three test stimuli using stimulating electrode ~50 µm far from the recording electrode. Test stimuli were given every 20 s, for 10 minutes before and 20 minutes after 100 Hz tetanic stimulation to measure the synaptic efficacy (Figure 17, F-J). **C**) Diagram of second recording electrode ~20 µm from stimulating electrode and ~200 µm from soma to excise an outside-out patch for fast Glutamate application **D**). **E**) Representative traces of AMPA receptor mediated Glutamate current (V_h=-80 mV) induced by 1 ms, 1 mM or 10 mM Glutamate. 1 mM Glutamate was used to measure kinetic properties (**Figure 20**) and current-voltage relationship of AMPA receptors (**Figure 21**). Cell-attached patch recordings from dendrites before and after tetanic

stimulation without **G**) and with **F**) NMDA receptor blockers evoked by three test stimuli. **H**) and **I**) show the integration of these capacitive currents (IC caused by evoked EPSPs) using the average of three traces to measure the synaptic efficacy change caused by tetanic stimulation. **J**) represents the change of synaptic efficacy measuring peak deflection after the first test stimulus in time before and after tetanic stimulation (see text, ** = P<0.01).

In our experiments we have investigated the impact of LTP induction on the properties of AMPA receptors on CA1 pyramidal neurons in the acute adult rat hippocampal slice. We excised outside-out patches from a region of the distal apical dendrite (~200 µm distal from soma) that presumably received incoming synaptic activity 20-30 min following a 100 Hz, 1 second tetanic stimulation (Magee & Johnston, 1997; Bannister & Larkman, 1995; Megias et al., 2001). Glutamate (1 and 10 mM) was then rapidly applied to the outside-out patches and AMPA receptor properties (single-channel conductance, open probability, receptor-channel kinetics, transmitter affinity and receptor numbers) were quantified. These data are compared with patch data acquired in an "unpotentiated" condition where NMDA receptor blockers were present to prevent synapse potentiation and with a control condition where no tetanic stimulation was given. We have found in patches pulled from potentiated cells that the AMPA receptor mediated glutamate current was increased in amplitude by nearly 75% (1019 ± 47 pA vs 1742 ± 173 pA; n=12, n=11) and that the current decay was slightly slowed compared to patches from the unpotentiated neurons (current half-width: control 13.8 ± 2.0 ms, n=7; unpotent. 14.6 ± 1.4 ms, n=12; LTP 20.8 ± 1.0 ms; n=11, P<0.01, **Figure 18**). A more detailed analysis follows.

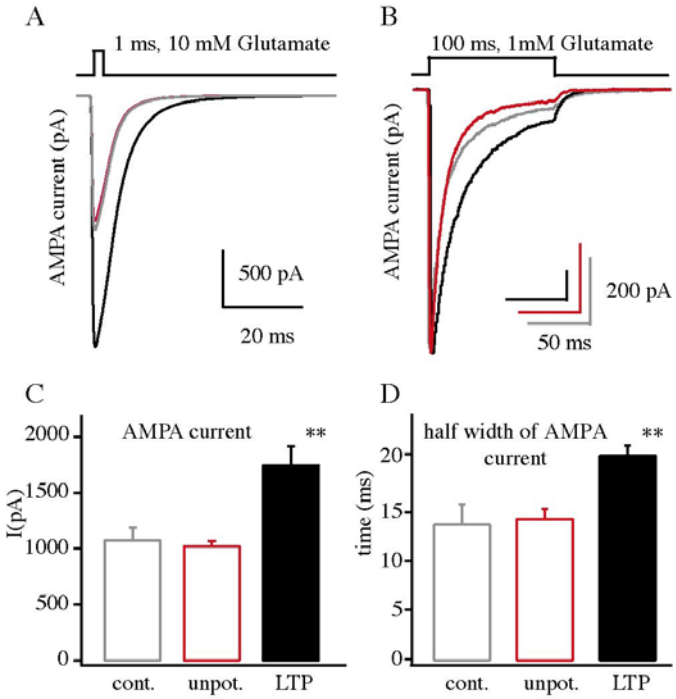

Figure 18. AMPA current changes following LTP. **A**) Representative average AMPA currents from patches pulled from

a control (gray), an unpotentiated neuron (50 μM APV and 10 μM MK-801, red) and a potentiated neuron (100 Hz tetanus, black) showing the increase in current amplitude that selectively occurs following LTP induction. **B**) Average AMPA currents evoked by 100ms 1mM glutamate application showing the increased current duration following potentiation. **C**) Represents numerically the AMPA current amplitude of patches excised from control (n=7), unpotentiated (n=12) and potentiated (n=11) neurons. **D**) Half width of AMPA currents quantifying the significant increase of AMPA current duration followed by LTP (** = P<0.01).

AMPA channel number

Sequential patch currents were submitted to a non-stationary fluctuation analysis (NSFA) to determine if the increased amplitude (**Figure 18**) of the AMPA currents observed following LTP was due to either an increase in channel number or to a change in single channel conductance (γ) or maximum probability of opening ($P_{o,max}$). The NSFA of currents from potentiated cells (**Figure 19**) showed that the number of AMPA receptors present in these patches was increased by 70% (1642 ± 126 vs 2771 ± 249; n=12, n=11), while the single-channel conductance (9.3 ±0.7pS vs 8.8 ± 0.9 pS), and channel maximum open probability (0.87 ± 0.03 vs 0.92 ± 0.01) were insignificantly increased. These data indicate that the larger amplitude currents present in potentiated patches are likely to be almost exclusively due to an increase in channel numbers and not to any changes in γ or $P_{o,max}$.

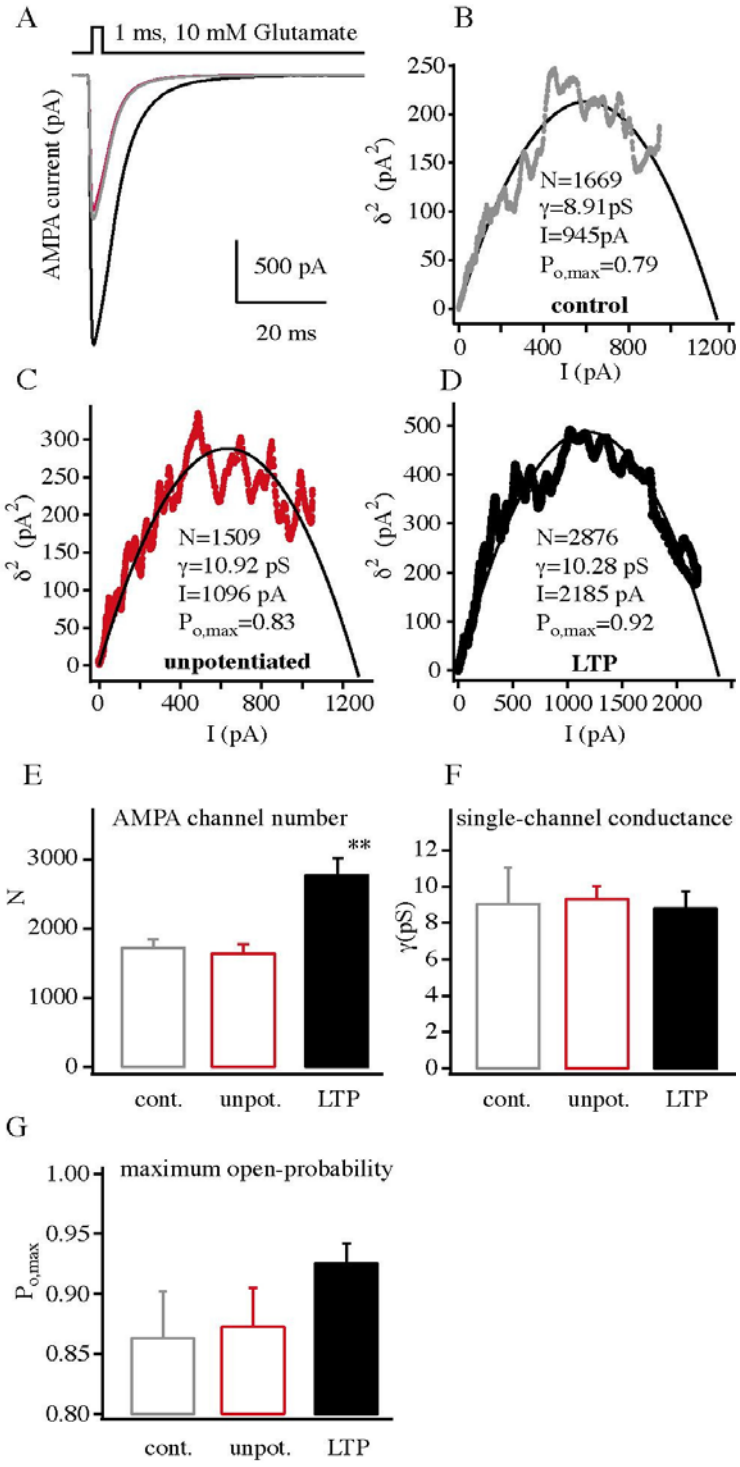

Figure 19. AMPA channel biophysical properties following LTP. **A**) Representative average AMPA currents from patches pulled from a control (gray), an unpotentiated neuron (50 µM APV and 10 µM MK-801, red), and a potentiated neuron (100 Hz tetanus, black). **B-D**) Plots of mean AMPA current versus variance that were used in non-stationary fluctuation analyses of the currents shown above. The number of channels in the patch (N), single channel conductance (γ), mean peak current amplitude (I) and maximum channel open probability ($P_{o,max}$) calculated from the fit of the plots by a parabolic function are shown (see methods). Pooled data of AMPA channel numbers (**E**) of dendritic excised patches from control (n=6), unpotentiated (n=12) and potentiated (n=11, ** = P<0.01). **F**) Single-channel conductance (γ) appears equal in every condition. **G**) The maximum open probability ($P_{o,max}$) shows a slight but statistically insignificant increase in the potentiated cells. The results of non-stationary fluctuation analysis suggest the channel number changes instead of the channel properties during potentiation. All dendritic outside-out patches were excised ~200 µm distal to the soma, 25-35 minutes after 100 Hz tetanic stimulation. 1ms, 10 mM Glutamate was used for maximal saturation of AMPA receptors for non-stationary fluctuation analysis.

Other channel properties

A more detailed analysis of the time course of AMPA receptor mediated glutamate currents revealed subtle changes in decay kinetics following potentiation that may underlie the observed current prolongation. Current rise-times after potentiation (0.58 ± 0.05; n=11) were identical with control (0.54 ± 0.04 ms; n=7) and unpotentiated (0.55 ± 0.05 ms; n=12) results. On the other hand, the time constant of channel deactivation was slightly increased following LTP induction (cont. 3.2 ± 0.3 ms, n=7; unpot. 4.1 ± 0.2 ms, n=10; pot. 4.4 ± 0.3 ms, n=11, P<0.05 vs control).

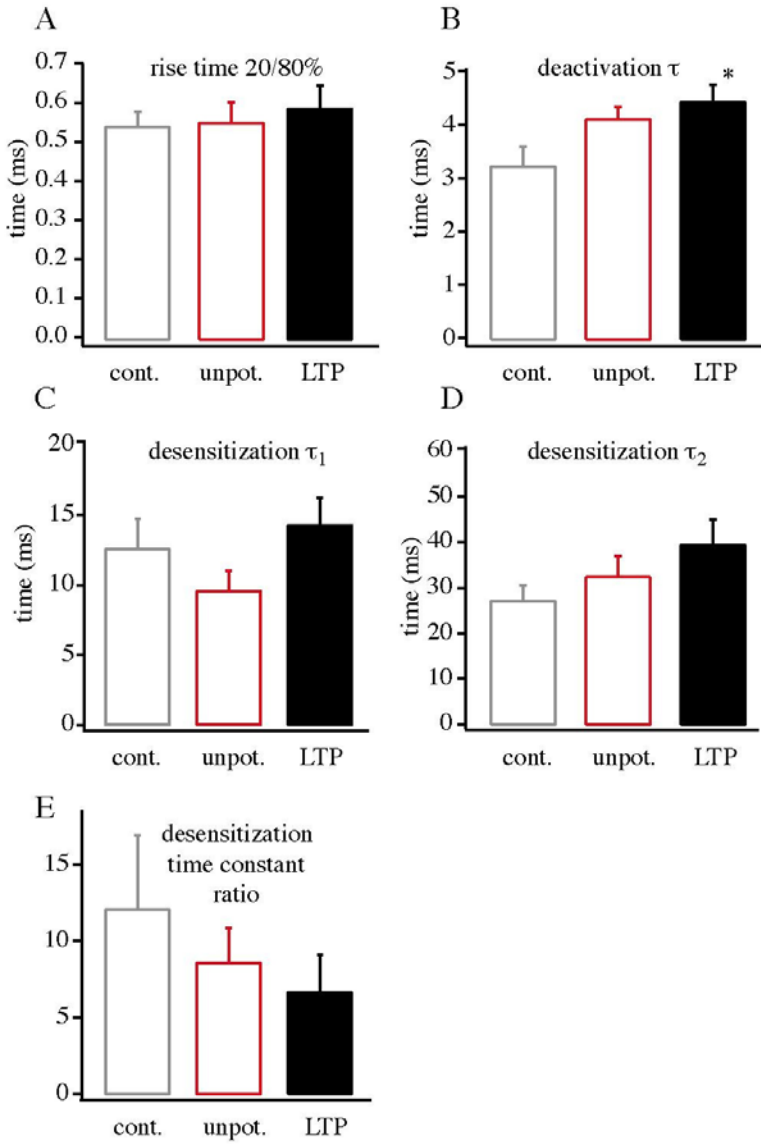

Figure 20. AMPA current kinetic changes following LTP. The kinetic properties of the AMPA receptor currents. **A**) rise time, **B**) deactivation time constant (τ), **C**) fast desensitization time constant (τ_1), **D**) slow desensitization time constant (τ_2), **E**) the desensitization time constant ratio. A slowing in kinetics can be seen during potetiation (n=11, LTP vs control, * = P<0.05).

The fast (τ_1) and slow (τ_2) desensitization time constants were not significantly increased after LTP (τ_1: cont. 12.5 ± 2.2 ms, n=7; unpot. 9.5 ± 1.4 ms, n=10; pot. 14.2 ± 1.9 ms, n=11) (τ_2: cont. 27.1 ± 3.4 ms, n=7; unpot. 32.4 ± 4.6 ms, n=10; pot. 39.4 ± 5.6 ms, n=11). Also, the ratio of fast to slow desensitization components was not significantly decreased following LTP induction (cont. 12.0 ± 4.8, n=7; unpot. 8.5 ± 2.3, n=10; pot. 6.6 ± 2.4, n=11) (**Figure 20**). We interpret these data to indicate that, although most of the changes in the individual kinetic parameters were in themselves statistically insignificant, the slight slowing observed in all of the measures of channel decay combine to produce a more prolonged AMPA current duration (half-width) following LTP induction.

AMPA channel rectification properties were also compared under control conditions and following LTP induction. A plot of the AMPA receptor mediated glutamate current amplitude versus holding potential (I/V)(from -80 mV to +80 mV, **Figure 21**) shows that LTP induction did not produce any changes in the rectification properties of the AMPA receptors in our patches. Finally, the ability of potentiation induction to produce a change in the glutamate affinity of the AMPA receptors in our patches was examined. To do so the ratio of 1 mM to 10 mM glutamate peak current amplitudes were compared between the three groups and was found to be unaltered. This data suggests that the glutamate affinity of these receptors didn't change for this range of concentrations (**Figure 21**). Together the data presented thus far suggest that the increase in AMPA receptor mediated current in patches from neurons showing synaptic potentiation is the result of an increase in AMPA receptor density in these synaptically active regions. It also appears that, other than a slight slowing of channel decay rates, there are no changes in the single-channel properties of the AMPA receptors responsible for the increase in patch current.

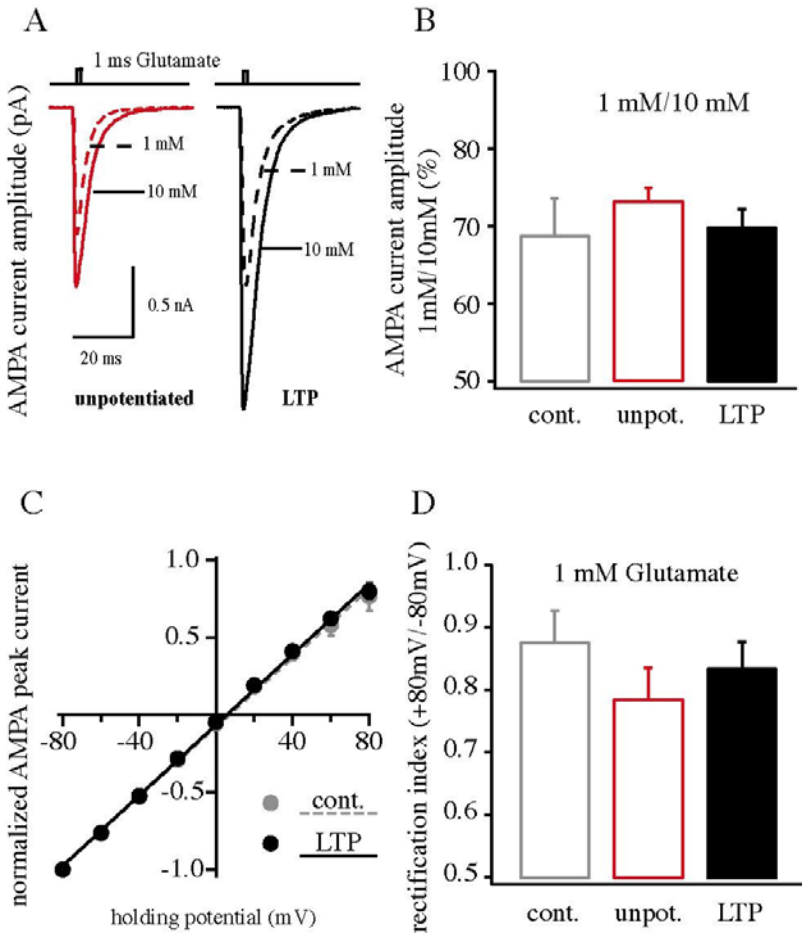

Figure 21. Potentiation does not change receptor affinity or channel rectification properties. **A**) shows representative traces of 1 mM and 10 mM glutamate (1 ms pulse) induced AMPA receptor mediated currents of excised dendritic patch from control (n=6), unpotentiated (n=12) and potentiated (n=11) cells. The ratio of 1 mM and 10 mM glutamate current **B**) are similar in all cases suggesting that the glutamate affinity of AMPA receptors did not change during potentiation. **C**) The current-voltage relationship of control (filled gray circle), LTP (filled black cicrcle,). The unpotentiated was similar (data not shown). **D**) The rectification index (peak current at +80/-80 mV) does not show any differences between these states.

CaMK-II activation increases AMPA currents

Earlier studies have suggested that calcium activated calmodulin kinase II (CaMK-II) mimics electrically evoked potentiation and that many of the changes in synaptic efficacy, including AMPA receptor single channel conductance and receptor cycling associated with LTP, are the result of increased CaMK-II activation (Wang & Kelly, 1995; Hayashi et al., 2000). We thus filled CA1 dendrites with high free Ca^{2+} and calmodulin (CaM) (4:1 ratio; Tao-Cheng et al., 2001) plus calcineurin autophosphorylation inhibitory peptide (CaN-AIP) (see Wang & Kelly, 1997) for 5-15 minutes to increase CaMK-II activity. Following this time, patches were excised, glutamate was rapidly applied as above and the AMPA receptor mediated currents were

analyzed as in the previous experiments. As with electrical stimulation these patch currents were larger in amplitude (1039 ± 43 pA vs 1765 ± 124 pA; n=7, n=10) because the number of AMPA receptors in the patches was increased (1726 ± 120 vs 3246 ± 454; n=7, n=10) while γ (9.1 ± 0.7 pS vs 7.2 ± 0.4 pS) and $P_{o,max}$ (0.86 ± 0.03 vs 0.91 ± 0.03) were unaltered.

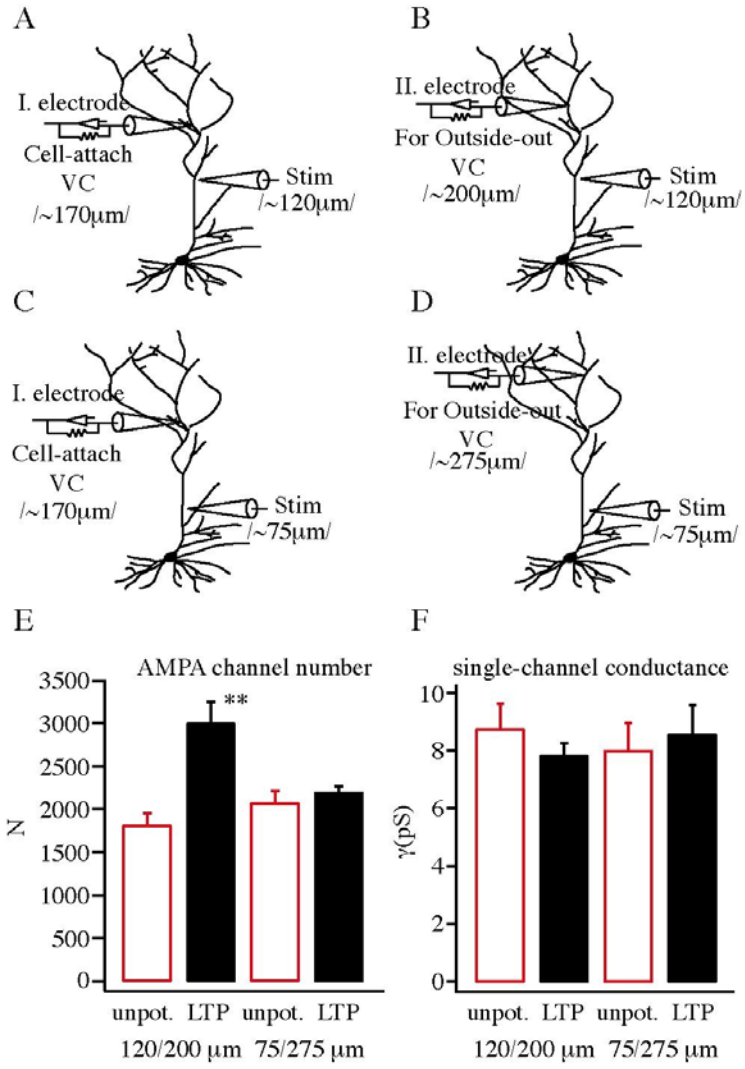

Figure 22. AMPA channel biophysical property changes following CaMK-II activation. **A**) Representative average AMPA currents from patches pulled from a control (gray), a CaMK-II activated neuron (20 mins Ca^{2+}/CaM, black) and AIP-blocked CaMK-II activated neuron (20 mins Ca^{2+}/CaM+AIP, red). **B-D**) Plots of mean AMPA current versus variance that were used in non-stationary fluctuation analyses of the currents shown above. The number of channels in the patch (N), single channel conductance (γ), mean peak current amplitude (I) and maximum channel open probability ($P_{o,max}$) calculated from the fit of the plots by a parabolic function are shown (see methods). Pooled data of AMPA channel numbers (**E**) of dendritic excised patches from control (n=7), CaMK-II (n=10), CaMK-II+AIP (n=6). **F**) Single-channel conductance (γ) appears equal in every condition. **G**) The maximum open probability ($P_{o,max}$) shows an insignificant increase in the CaMK-II activated cells. The results of non-stationary fluctuation analysis suggest the channel number changes instead of the channel properties during potentiation. All dendritic outside-out patches were excised ~200 μm distal to the soma, 20-30 minutes Ca^{2+}/CaM intracellular application. 1ms, 10 mM Glutamate was used for maximal saturation of AMPA receptors for non-stationary fluctuation analysis (** = P<0.01).

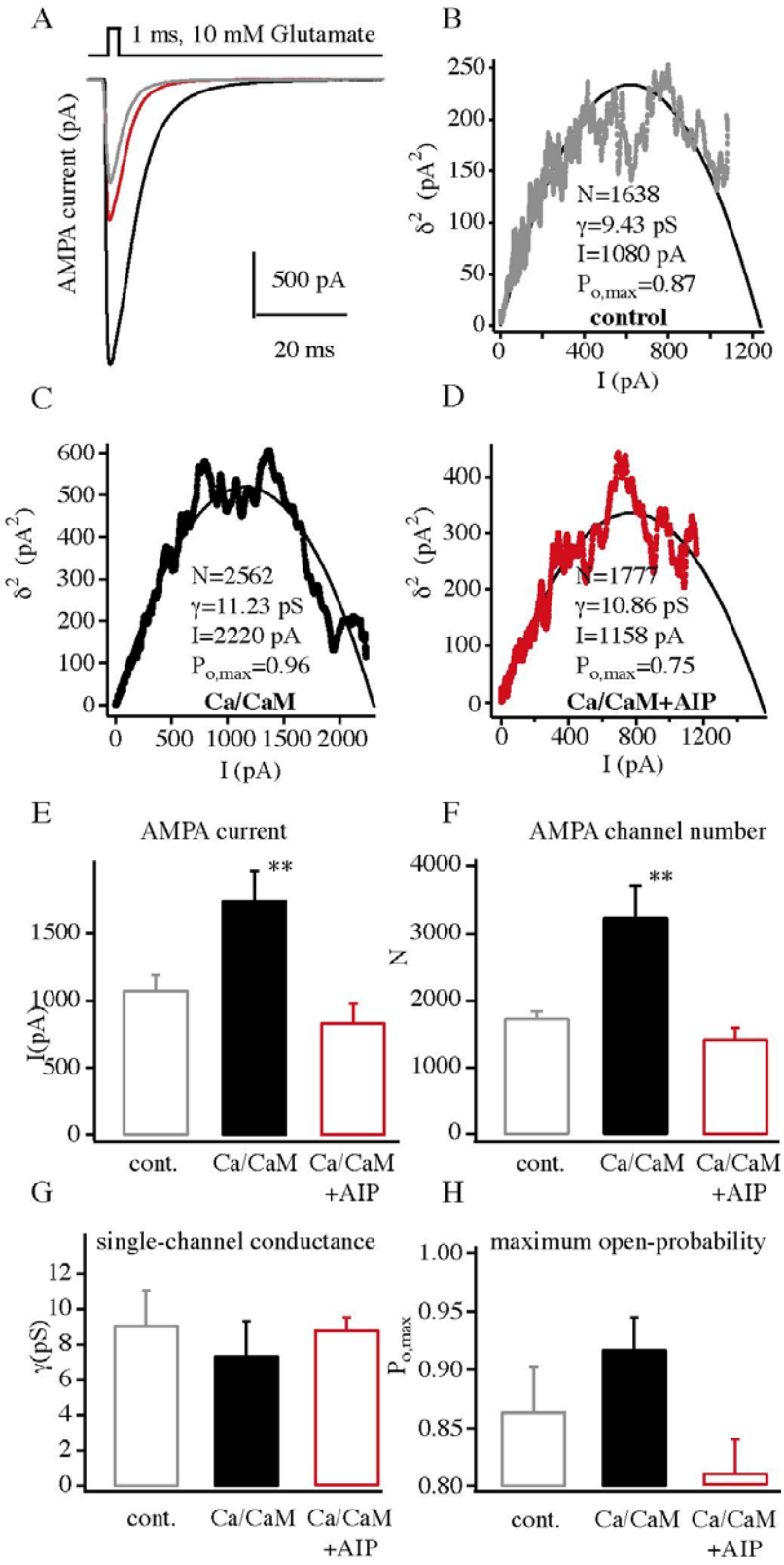

Figure 23. AMPA current kinetic changes following CaMKII activation. The kinetic properties of the AMPA receptor current; **A**) rise time, **B**) deactivation time constant (τ), **C**) fast desensitization time constant (τ_1), **D**) slow desensitization time constant (τ_2), **E**) the desensitization time constant ratio of dendritic excised patches from control (n=7), CaMK-II (n=10), CaMK-II+AIP (n=6). A slowing in kinetics can be seen during Ca/CaM treatment. AIP application with Ca/CaM shows the same values as in control. **F**) Half width of AMPA currents demonstrate the increase of AMPA current decay followed by CaMK-II activation (** = P<0.01).

Additionally, the increase in CaMK-II activity produced a similar AMPA current kinetic profile as electrical stimulation. Here, we again observed a slight but significant change in channel deactivation, but only insignificant slowing of the various desensitization parameters (see **Figure 24**). Finally, inclusion of 1 µM autophosphorylation inhibiting protein (AIP, n=6) in the pipette prevented all of the alterations produced by CaMK-II activation (see **Figure 22, 23**). These data indicate that, as in other studies, CaMK-II activation can mimic the effects of electrically evoked synaptic potentiation. They furthermore, suggest that native AMPA receptors in hippocampal CA1 pyramidal neurons do not respond to increased CaMK-II activity with an increase in γ but instead with a increase in channel density.

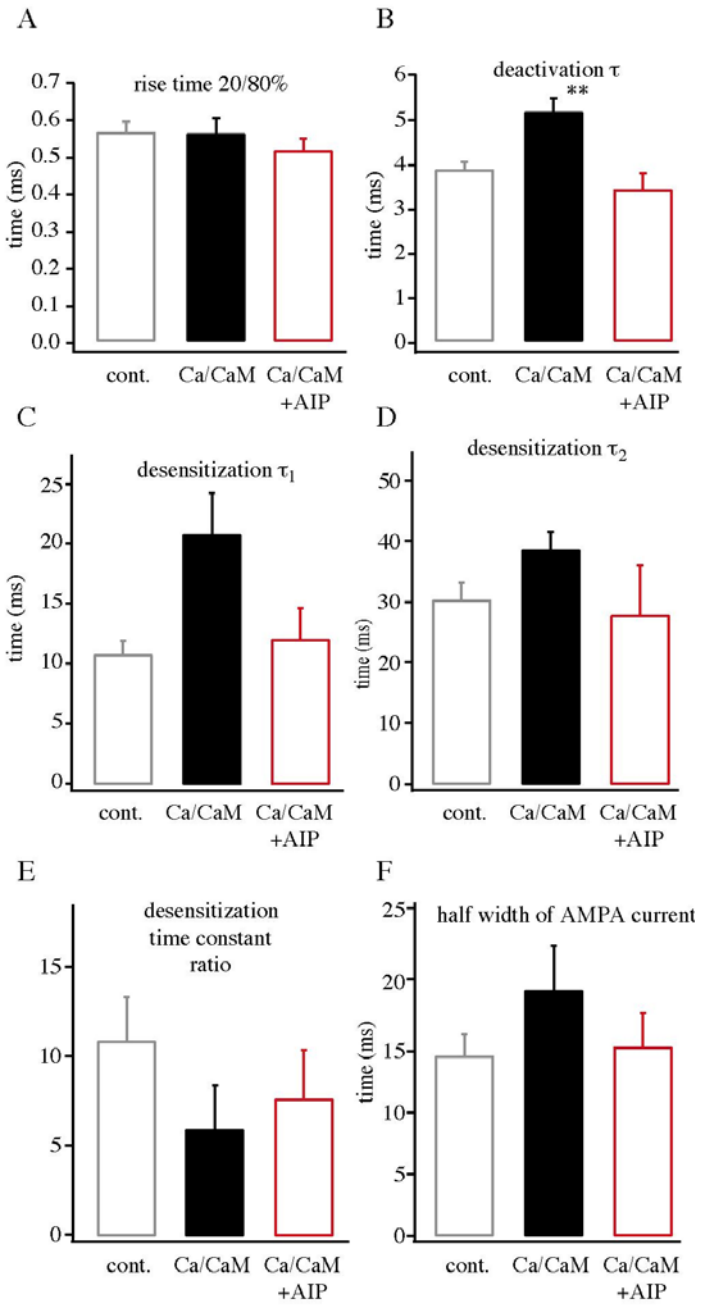

Figure 24. Regionalization of AMPA receptor changes. **A,B** the experimental configuration for pulling the outside-out patch near the site of the LTP induction (80-100 µm distal to the stimulation site). **C,D**) Show the experimental configuration for pulling patches at a site that was distant to the stimulation site (~200 µm distant). Pooled data (LTP n=4, unpotentiated n=3) show that AMPA channel number (**E**) is increased when the patch was pulled near the site of stimulation but not when it was far away. There were no changes in single-channel conductance under any conditions.

Dendritic region showing AMPA current potentiation

Next we wanted to monitor the spatial extent of the increase in patch AMPA currents in the apical dendrite following the strong electrical stimulation we were using. To do so we excised outside-out patches at different distances from the stimulation and recording sites (see **Figure 24**). In summary, we could detect a large increase in AMPA channel numbers (1804 ± 146 vs 2988 ± 252) for up to 80 μm away from the stimulation site (patch site: 200 ± 20 μm from soma; stimulation site: 120 ± 20 μm from soma). We did not, however, observe any such changes (2060 ± 148 vs 2185 ± 80) when the patch was pulled from greater distances away from the stimulation site (patch site: 275 ± 20 μm; stimulation site: 75 ± 20 μm). These data suggest that while the potentiation did affect a large part of the dendrite (~150 μm), it did not affect all of the arborization (**Figure 24**). In fact we suspect that the dendritic region affected by the stimulation is not much larger than the region receiving synaptic stimulation (see methods), especially considering the less than precise localization of LTP induction (Engert & Bonhoeffer, 1997).

Are synapses and or dendritic spines required for the LTP associated increases in AMPA receptor currents? To investigate this question we activated CaMK-II in the proximal dendritic region (only ~20 μm away from soma) where there are virtually no excitatory synapses (Bannister & Larkman, 1995; Megias et al., 2001). After 5-15 min filling this region of the dendrite with our high Ca/CaM containing solution, outside-out patches were excised and the standard AMPA current analyses produced. In contrast to what was observed above at synaptically dense regions of the dendrite, we did not see any increases in AMPA current in the patches pulled from this region of the dendrite (491 ± 116 pA vs 479 ± 144 pA; n=9, n=7). Furthermore, NSFA showed that there was no increase in AMPA channel number or any alteration in single channel properties (**Figure 25**). These observations strongly suggest that the underlying machinery of increasing AMPA channel number in the sub- and/or extrasynaptic membrane must be related somehow to the special synaptic or spine structures.

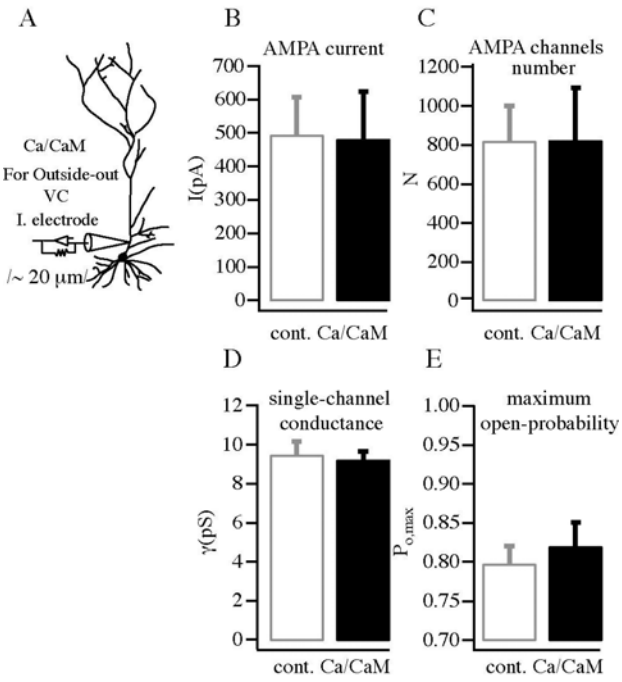

Figure 25. Synaptic structures are required for the increase in AMPA channel numbers caused by CaMK-II activation. A) Intracellular application of Ca/CaM (n=7) at the proximal part of the apical dendrites (~20 μm away from soma) did not have an impact on (control n=9) any properties of excised AMPA receptors, B-D), suggesting the localization dependence of phosphorylation governs receptor insertion or lateral transportation.

Discussion

Summary

In recent years many attempts have been made to clarify the mechanisms by which synaptic efficacy is increased following the induction of LTP. In this study we have characterized the changes in dendritic AMPA receptors in hippocampal CA1 pyramidal neurons from adult rats that are produced by, or at least coincide with, LTP induction. The main observations are 1) tetanus induced potentiation significantly increased the amplitude of AMPA receptor mediated glutamate currents in outside-out patches pulled from the apical dendrites of adult rats. 2) This increase is due to an increase in the number of AMPA receptors in the patches. 3) AMPA currents from potentiated dendritic regions also decay more slowly, but there was no single kinetic parameter responsible for this slowing. 4) Other properties of AMPA receptors such as single-channel conductance, channel rectification and glutamate affinity do not show any alterations following potentiation. 5) Increases in intracellular CaMK-II activity mimic the changes in AMPA receptor properties that were observed following tetanus-induced potentiation. 6) The dendritic region affected by the synaptic stimulation is not much greater than the area

receiving input and requires the presence of excitatory synapses. We interpret our data to indicate that the stimuli used here produce an increased delivery of AMPA receptors to synaptically-active regions of the apical dendrite without inducing any significant changes in their basic biophysical properties. We suspect that the primarily extra-synaptic receptors sampled by our patches (see below) will ultimately arrive at activated PSDs via the regulated process of receptor cycling between the synaptic and extra-synaptic pools of AMPA receptors.

Origin of AMPA receptors

In our previous work (Andrásfalvy et al., 2003) we made an effort to determine the origin of the excised receptors on outside-out patches, using GluR1 -/- mice. In these mice there is a nearly complete (~97%) loss of AMPA receptor currents in outside-out patches from both spiny (synaptic) and non-spiny (non-synaptic) regions, while purely synaptic currents (mEPSCs) are reduced only ~30% at proximal locations. That AMPA receptor patch currents are equally reduced in both spiny and non-spiny regions of GluR1 -/- mice suggests that either the receptors in outside-out patches are from extra-synaptic regions or that synaptic and extra-synaptic currents were both equally reduced in these mice. However, the observation that synaptic currents (mEPSCs) are, in fact, much less reduced than outside-out patch currents (30% vs 97% reduction), leaves us to conclude that the AMPA receptors in our outside-out patches are mostly from extra-synaptic regions. These extra-synaptic regions could be either the dendrite trunk or the non-synaptic regions of spines (Andrásfalvy et al., 2003). A probable explanation for this result is that the very tight connection between the post-synaptic density (PSD) and the active zone (AZ) membrane at the synapse proper does not allow the receptors located there to be readily pulled into outside-out patches, while other receptors nearby the PSD are available. We thus conclude that LTP induction in CA1 pyramidal neurons leads to an increase in the extra-synaptic pool of AMPA receptors in dendritic regions near activated synapses.

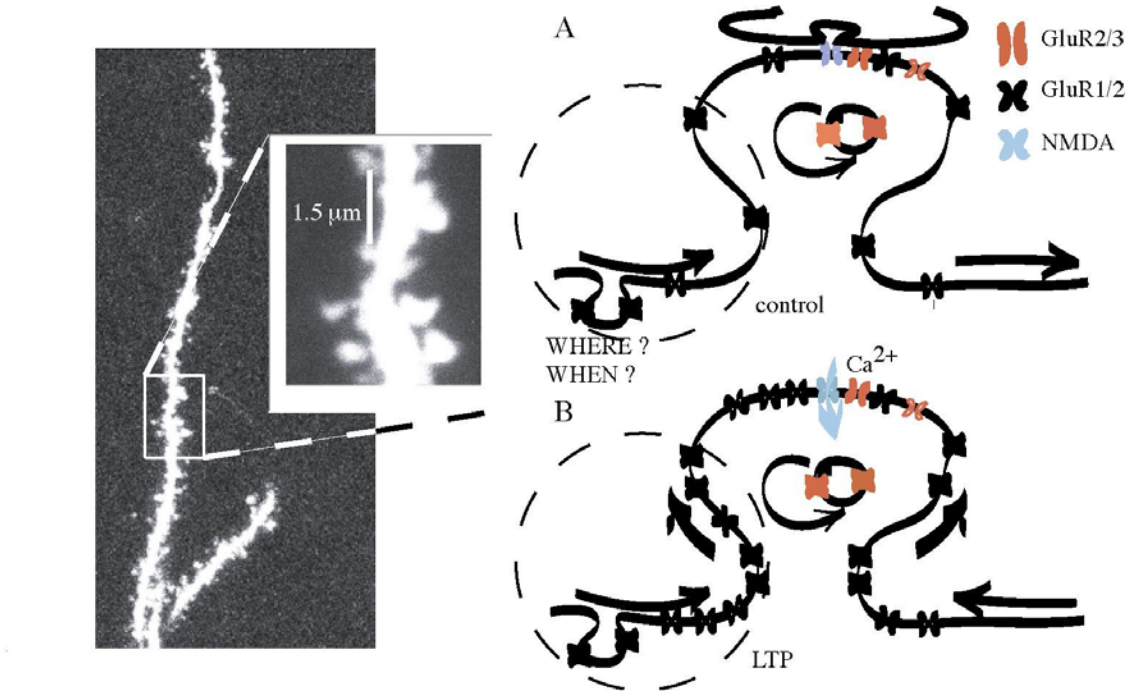

Figure 26. Model of AMPA receptor redistribution or transportation into the subsynaptic and synaptic area during LTP induction in adult hippocampal neurons. The picture shows a distal apical dentritic trunk and on the magnified insert the scale bar indicates the average tip aperture of our pipettes. A) the dashed circle indicates the putative outside-out patch membrane area containing extrasynaptic and sub- or juxtasynaptic AMPA receptors. Under resting conditions the GluR2/3 (red) AMPA receptors are continuously exo- and endocytosed directly into the PSD. Most of the GluR1/2 AMPA receptors (black) are mobile in the extra- and subsynaptic area and continuously moving in and out of the PSD by lateral drift, but are not anchored there. B) When Ca^{2+} flows through NMDA ion channels (blue) during depolarization, many phosphorylation cascades are initiated, which activate transporting- and anchoring proteins. The mobile GluR1/2 receptors move towards the PSD and are anchored there. Lateral drift of more extrasynaptic receptors makes more receptors available in the sub- or juxtasynaptic region. The number of GluR1/2 receptors in this region mirrors the increase in synaptic AMPA receptors.

AMPA receptor cycling and delivery during synaptic plasticity

Previous studies have demonstrated differently regulated incorporation of subunit-specific AMPA receptors into synapses as one underlying mechanism of various synaptic plasticity phenomena (Shi et al., 2001; Kim et al., 2001; Lu et al., 2001; Piccini & Malinow, 2002; Passafaro et al., 2001; Heynen et al., 2000; Grosshans et al., 2002). In these schemes, GluR2/3 receptors are thought to be delivered directly into the synapse and continuously recycled within the synapse through exo- and endocytosis (Shi et al., 2001; Kim et al.,

2001; Meng et al., 2003). GluR1/2 receptors are thought to initially insert into the extra-synaptic membrane and then move laterally into the postsynaptic density depending on the activity pattern of the synapse (Chen et al., 2000; Lu et al., 2001; Passafaro et al., 2001; Piccini & Malinow, 2002; Andrásfalvy et al., 2003; Zamanillo et al., 1999; Mack et al., 2001; Shi et al., 2001; Meng et al., 2003; but see Hoffman et al., 2002). Thus, a baseline of synaptic efficacy is thought to be established by GluR2/3 receptors, with the regulated delivery of GluR1/2 receptors either directly or indirectly increasing synaptic weight depending upon the associative history of the synapse.

In this work, we have shown that the decay times of AMPA receptor mediated glutamate currents have increased and that $P_{o,max}$ did not decrease following synaptic potentiation. Based on our previous observations (Andrásfalvy et al., 2003) that AMPA currents from GluR1-deficient mice (probably GluR2/3) decay faster and have a lower $P_{o,max}$ than AMPA currents from wild-type mice (probably GluR1/2), we suggest that the increased amount of AMPA receptors present in the potentiated patches are mediated by GluR1/2 AMPA receptors. This idea meshes nicely with the idea that it is the GluR1 containing AMPA receptors that are delivered to the synapses in an activity-dependent manner.

Exocytosis or cluster formation and lateral drift of extrasynaptic receptors into synapses

NMDA receptor trafficking through lateral diffusion in and out of synapses has been shown (Tovar & Westbrook, 2002). Furthermore, Choquet and his colleagues (Tardin et al., 2003) have reported that half of the GluR2 containing synaptic receptors are mobile and this mobility is affected by pharmacological treatments that modify receptor accumulation at synapses (O'Brien et al., 1998). Their results suggested a dynamic equilibrium between the extrasynaptic and synaptic receptor pools, supporting the idea that the regions around synapses form a reserve pool zone and transition area, providing available receptors for recruitment at synapses. Our previous work has also suggested that the number of AMPA receptors in excised outside-out patches (from mostly subsynaptic & extrasynaptic regions) is proportional to the synaptic receptor pool, lending support to the concept that any changes in the size of one pool will be manifested in the other (Andrásfalvy & Magee, 2001; Smith et al., 2003; Andrásfalvy et al., 2003). Therefore our

data suggest that an increase in the number of AMPA receptors present in the reserve receptor pool (either through lateral diffusion or regulated exocytosis) is one important event that occurs following the induction of LTP in CA1 pyramidal neurons. We would also expect that these additional receptors would then be available to find their way, through interactions with transporting (stargazin, GRIP, etc) and scaffolding/anchoring (actin, PSD, etc.) proteins, to synapses that had been activated during the LTP inducing stimulation.

Conclusion

How does the nervous system encode information, and what experience induced cellular mechanisms are capable of modifying the properties of a neuronal network?

Currently, the most widely accepted theory of remembering neuronal network is the idea of changing excitatory and inhibitory synaptic connections. They can be weakened or strengthened by different input patterns, which affects integration and changes the neuronal activity and excitability. These changes can last for minutes, hours or even weeks. The excitatory synaptic transmission is conveyed by presynaptically released glutamate acting on postsynaptic receptors (AMPA, NMDA, Kainate). Recent work suggested that changes in the properties or/and number of these glutamatergic receptors could be the basis of certain type of synaptic plasticity.

AMPA receptors are heteromeric or homomeric channels built from subunits GluR1-4. Recently, several details of transport and insertion of different types of heteromeric AMPA receptor have been described, including the different physiological roles of different subunits as determined mostly by their C-termini, where different phosphorylation, transport and anchor protein binding sites are located.

In single mammalian neurons, thousands of mixed excitatory and inhibitory synaptic inputs dynamically change their synaptic weights and/or influence the intrinsic properties of the neuron according to the history of the events and the input/output relationship. Recently, we were able to refine the electrophysiological recording technique of local synaptic activity and applied it to rats and mice where genetic manipulations can be made. I have directly examined single synaptic transmission before

and after different electrical/molecular manipulations in control and genetically modified mice, avoiding the spatial and temporal influence of other synapses and/or anatomically uneven dendritic conductance differences that distort conventional somatic recordings. Previous studies strongly suggest that different subunit combinations of AMPA receptors are differentially involved in the three types of plasticity (I. Homeostatic, II. Hebbian-type and III. Distance-Dependent-Synaptic-Scaling) and offer a great opportunity to investigate them by manipulation of the receptor subunits.

Homeostatic plasticity provides network and cellular stability, globally optimizes synaptic connections and regulates excitability, adjusting the gain of neurons in a dynamically changing environment. Hebbian type plasticity (LTP, LTD, etc) produces associative changes in individual synaptic strength and progressively modifies network properties by, increasing synaptic weight differences between synapses (depending on synaptic event history). It is believed that this is crucial for computational tasks, learning and memory. Distance dependent synaptic scaling (DDSS) adjusts the weight of every synapse to make them equally capable of having the same impact on output regardless of their distance from the soma.

At first, in our investigation I focused on the apical dendrites of CA1 pyramidal neurons, innervated by the Schaffer collaterals coming from the CA3 neurons. The Schaffer collateral pathway provides hippocampal CA1 pyramidal cells with a fairly homogeneous excitatory synaptic input that is spread out across several hundred microns of their apical dendritic arborizations. A progressive increase in synaptic conductance with distance from the soma has been reported to reduce the location-dependence that should result from this arrangement. By excising outside-out patches from apical dendrite and rapidly applying glutamate to activate AMPA and NMDA channels, I have characterized the amplitude, agonist affinity, kinetics and single channel properties of glutamate receptor-mediated currents, and compared these properties on patches excising from different locations from the apical dendrites of CA1 pyramidal neurons. The main finding is that the mean amplitude of the AMPA current at least doubles with distance from the soma. This distance-dependent increase in AMPA receptor current could be the result of an increased receptor number, receptor density or some modification of receptor properties. Modified subunit composition or different phosphorylation states can change

the kinetic properties, ionic permeability, agonist affinity, current-voltage relationship, single-channel conductance and maximum open-probability of AMPA channels. We examined all of these receptor properties and compared them with distance from the soma, and found no significant differences in any of them, while on the other hand, channel number increased approximately two-fold. These data then strongly suggest that the distance dependent increase in AMPA current is due to a progressive increase in number of AMPAR in the patches and not to alterations in the basic properties of the receptor/channels.

In the second part of our investigation, we have characterized the properties of dendritic AMPA receptors, spontaneous synaptic currents and postsynaptic AMPA receptor responsiveness in hippocampal CA1 pyramidal neurons from both wild type and GluR1 -/- mice. The AMPA receptor currents from outside-out patches pulled from apical dendrites of GluR1 -/- mice are severely reduced in amplitude. The currents from the KO mice also appear to decay faster and have a lower probability of opening than WT currents. Spontaneous synaptic currents are also smaller in amplitude in the KO mice and the degree of this reduction is dependent on the dendritic location of the synapse, with distal synapses showing the greatest reduction. Statistical analyses of the synaptic currents indicate that the distal SC synapses of KO mice lack a normal increase in postsynaptic responsiveness, and focal application of glutamate onto postsynaptic spines confirms this scenario. We interpret these data to indicate that the extra-synaptic pool of AMPA receptors is almost entirely composed of GluR1-containing AMPA receptors (probably GluR1/2 heteromeres) and that distance-dependent scaling of SC synaptic weight is the result of an increased delivery of these receptors to distal synapses. Furthermore, this regulated delivery probably involves receptor cycling of AMPA receptors between the synaptic and extra-synaptic pools.

The third part of our study examined the changes in dendritic AMPA receptors in hippocampal CA1 pyramidal neurons from adult rats that are produced by, or at least coincide with, LTP induction. Tetanus induced potentiation significantly increased the amplitude of AMPA receptor mediated glutamate currents in outside-out patches pulled from the apical dendrites of adult rats. This increase is due to an increase in the number of AMPA receptors in the patches. These currents also appear to decay more slowly and

have a slightly higher probability of opening than control or unpotentiated neurons. Other properties of AMPA receptors, such as single-channel conductance, channel rectification and glutamate affinity do not show any alterations following potentiation. Increases in intracellular CaMKII activity mimic the changes in AMPA receptor properties that were observed following tetanus-induced potentiation. The dendritic region affected by the synaptic stimulation is not much greater than the area receiving input and requires the presence of excitatory synapses. We interpret our data to indicate that the stimuli used here produce an increased delivery of AMPA receptors (probably GluR1/2 heteromers) to synaptically-active regions of the apical dendrite without inducing any significant changes in their basic biophysical properties. We suspect that the primarily extra-synaptic receptors sampled by our patches will ultimately arrive at activated PSDs via the regulated process of receptor cycling between the synaptic and extra-synaptic pools of AMPA receptors.

All of our results are compressed into a simplified model, indicating that the changes in number and/or properties of AMPA receptors are the crucial underlying mechanism of different forms of synaptic plasticity, and that certain types of subunit composed channels are differentially involved. The GluR1 containing AMPA receptors are a basic component of the synaptic pool of glutamate receptors at Schaffer-collateral synapses, particularly at distant synapses. Also GluR1 containing AMPA receptors are the main component of the extra-synaptic AMPA receptor pool. In addition Location-dependent insertion of GluR1 containing AMPA receptors mediates distance-dependent scaling in hippocampal CA1 pyramidal neurons. Together these data suggest that the highly regulated cycling of AMPA receptors between synaptic and extra-synaptic receptor pools is dependent upon the presence of GluR-1 containing receptors, and furthermore that two functionally diverse forms of synaptic plasticity, LTP and distance-dependent scaling, may both use this cycling system to regulate synaptic strength. Also, the lack of GluR1 subunits in KO animals suggests that every synapse is formed by roughly the same number of GluR2/3 subunits regardless of distance from soma. This observation indirectly suggests, that GluR1 containing receptors are added to ″top-up″ synapses depending on their distance from the soma. On the top of these distance scaled synapses, more GluR1 containing receptor can be added during long-term potentiation. It

is certain that, these plasticity forms have an affect on each other and do not work separately to maintain the homeostasis of the neuronal network and retain the ability to react properly in a dynamically changing environment.

Acknowledgements

I am most grateful to Dr. Jeffrey C. Magee for his support, teaching me high level electrophysiology, providing excellent laboratorial environment, believing in my ideas and letting them to be tried. I also have to thank to my colleagues; Dr. Sonia Gasparini, Dr. Mark A. Smith and Carmel McDermott for their help.

I am grateful to my wife for her loving patience and support.

References

Alvarez FJ, Dewey DE, Harrington DA & Fyffe RE (1997). Cell-type specific organization of glycine receptor clusters in the mammalian spinal cord. *J Comp Neurology* **379**:50-70.

Andrásfalvy BK & Magee JC (2001). Distance-dependent increase in AMPA receptor number in the dendrites of adult hippocampal CA1 pyramidal neurons. *J Neurosci*. **21**:9151-9159.

Andrásfalvy BK & Magee JC AMPA (2002). Channel density and properties change following Ca/CaM treatment in CA1 pyramidal neurons. *Soc Neurosci Abstracts* **32**:713.7

Andrásfalvy BK, Smith MA, Borchardt T, Sprengel R & Magee JC (2003) Impaired regulation of synaptic strength in hippocampal neurons from GluR1-deficient mice. *J Physiol.* **552**:35-45.

Archibald K, Molnár E & Henley JM (1999) Differential changes in the subcellular distribution of α-amino-3-hydroxy-5-methyl-4-isoxazole propionate and *N*-methyl-D-aspartate receptors in neonate and adult rat cortex. *Neurosci Lett* **270**:49-52.

Banke TG, Bowie D, Lee H-K, Huganir RL, Schousboe A, Traynelis SF (2000) Control of GluR1 AMPA receptor function by cAMP-dependent protein kinase. *J Neurosci* **20**:89-102.

Bannister NJ, Larkman AU (1995) Dendritic morphology of CA1 Pyramidal neurons from the rat hippocampus: II. Spine distribution. *J Comp Neurology* **360**:161-171.

Benke TA, Lüthi A, Isaac JT & Collingridge GL (1998). Modulation of AMPA receptor unitary conductance by synaptic activity. *Nature* **393**:793-797.

Bliss TV & Collingridge GL (1993) A synaptic model of memory: long-term potentiation in the hippocampus. *Nature* **361**:31-39.

Bolshakov VY, Golan H, Kandel ER, Siegelbaum SA (1997) Recruitment of new sites of synaptic transmission during the cAMP-dependent late phase of LTP at CA3- CA1 synapses in the hippocampus. Neuron 19:635-646.

Burrone J, O'Byrne M & Murthy VN (2002). Multiple forms of synaptic plasticity triggered by selective suppression of activity in individual neurons. *Nature* **420**:414-418.

Bykhovskaia M, Hackett JT, Worden MK (1999) Asynchrony of quantal events in evoked multiquantal responses indicates presynaptic quantal interaction *J. N*europhysiol **81**:2234-2242.

Chen C, Magee JC, Marcheselli V, Hardy M & Bazan NG (2001). Attenuated long-term potentiation in hippocampal dentate gyrus neurons of mice deficient in the platelet-activating factor receptor. *J Neurophysiol* **85:**384-390.

Chen L, Chetkovich DM, Petralia RS, Sweeney NT, Kawasaki Y, Wenthold RJ, Bredt DS & Nicoll RA (2000). Stargazin regulates synaptic targeting of AMPA receptors by two distinct mechanisms. *Nature* **408**:936-943.

Clements JD, Lester R AJ, Tong G, Jahr CE, Westbrook GL (1992) The time course of glutamate in the synaptic cleft. Science **258**:1498-1501.

Colbert CM, Johnston D (1996) Axonal action-potential initiation and Na^+channel densities in the soma and axon initial segment of subicular pyramidalneurons. *J Neurosci* **16**:6676-6686.

Colquhoun D, Jonas P, Sakmann B (1992) Action of brief pulses of glutamate on AMPA/kainate receptors in patches from different neurons of rat hippocampal slices. *J. Physiol* **458**:261-287.

Davis GW, Bezprozvanny I. (2001) Maintaining the stability of neural function: a homeostatic hypothesis. Review. *Ann. Rev. Physiol.* **63**:847-869.

Derkach V, Barria A & Soderling TR (1999). Ca2+/calmodulin-kinase II enhances channel conductance of alpha-amino-3-hydroxy-5-methyl-4-isoxazolepropionate type glutamate receptors. *Proc Natl Acad Sci U S A* **96**:3269-3274.

Dingledine R, Borges K, Bowie D, Traynelis SF (1999) The glutamate receptor ion Channels. *Am Soc Pharmacol Exp Therap* **51**:7-61.

Dingledine R, Botges K, Bowie D & Traynelis SF (1999). The glutamate receptor ion channels. *Pharmacol Rev* **51**:7-61.

Dudek SM & Bear MF (1993) Bidirectional long-term modification of synaptic effectiveness in the adult and immature hippocampus. *J Neurosci* **13**:2910-2918.

Engert F & Bonhoeffer T (1997) Synapse specificity of long-term potentiation breaks down at short distances *Nature* **388**:279-284.

Frick A, Magee JC, Johnston D (2004) LTP is accompanied by an enhanced local excitability of pyramidal neuron dendrites. *Nat Neurosci* **7**:1-10.

Frick A, Zeigelgansberger W, Dodt HU (1998) *Soc Neurosci Abstracts* **24**:325.

Furuyama T, Kiyama H, Sato K, Park HT, Maeno H, Takagi H & Tohyyama M (1993). Region-specific expression of subunits of ionotropic glutamate receptors (AMPA-type, KA-type and NMDA receptors) in the rat spinal cord with special reference to nociception. *Mol Brain Res* **18**:141-151.

Geiger JRP, Lübke J, Roth A, Frotscher M & Jonas P (1997). Submillisecond AMPA receptor-mediated signaling at a principal neuron-interneuron synapse. *Neuron* **18**:1009-1023.

Greengard P, Jen J, Nairn AC, Stevens CF (1991) Enhancment of the glutamate response by cAMP-dependent protein kinase in hippocampal neurons. *Science (Wash DC)* **253**:1135-1138

Grosshans DR, Clayton DA, Coultrap SJ, Browning MD (2002) LTP leads to rapid surface expression of NMDA but not AMPA receptors in adult rat CA1. *Nat Neurosci* **5**:27-33.

Hayashi Y, Ishida A, Katagiri H, Mishina M, Fujisawa H, Manabe T, Takahashi T. (1997) Calcium- and calmodulin-dependent phosphorylation of AMPA type glutamate receptor subunits by endogenous protein kinases in the post-synaptic density. *Brain Res Mol Brain Res* **46**:338-342.

Hayashi Y, Shi SH, Esteban JA, Piccini A, Poncer JC & Malinow R (2000). Driving AMPA receptors into synapses by LTP and CaMKII: requirement for GluR1 and PDZ domain interaction. *Science* **287**:2262-2267.

Heynen AJ, Quinlan EM, Bae DC & Bear MF (2000) Bidirectional, activity-dependent regulation of glutamate receptors in the adult hippocampus in vivo. *Neuron* **28**:527-536.

Hoffman DA, Sprengel R & Sakmann B (2002). Molecular dissection of hippocampal theta-burst pairing potentiation. *Proc Natl Acad Sci USA* **99**:7740-7745.

Inasek R & Redman SJ (1973). The amplitude, time course and charge of unitary excitatory post-synaptic potentials evoked in spinal motorneurone dendrites. *J Physiol (Lond)* **234**:665-688.

Jack JJ, Redman SJ (1971) The propagation of transient potentials in some linear cable structures. *J Physiol.* **215(2)**:283-320.

Jaffe DB, Carnevale NT (1999) Passive normalization of synaptic integration influenced by dendritic architecture. *J Neurophysiol* **82(6)**:3268-3285.

Jonas P, Sakmann B (1991) Glutamate receptor channels in isolated patches from CA1 and CA3 pyramidal celld of the rat hippocampus slice. *J Physiol* **455**:143-171.

Keinänen K, Wisden W, Sommer B, Werner P, Herb A, Verdoorn TA, Sakmann B, Seeburg P (1990) A family of AMPA-selective glutamate receptors. *Science* **249**:556-560.

Kim CH, Chung HJ, Lee HK & Huganir RL (2001). Interaction of the AMPA receptor subunit GluR2/3 with PDZ domains regulates hippocampal long-term depression. *Proc Natl Acad Sci U S A* **98**:11725-11730.

Knapp AG, Schmidt KF, Dowling JE (1990) Dopamine modulates the kinetics of ion channels gated by excitatory amoni acids in retinal horizontal cells. *Proc Natl Acad Sci* **87**:767-771.

Korn H, Bausela F, Carpier S & Faber DS (1993). Synaptic noise and multiquantal release at dendritic synapses. *J Neurophysiol* **70**:1249-1253.

Larkman AU, Jack JJ, Stratford KJ (1997) Quantal analysis of excitatory synapses in rat hippocampal CA1 in vitro during low-frequency depression. *J. Physiol. (Lond.)* **505**:457-472.

Lisman J, Schulman H & Cline H (2002) The molecular basis of CaMKII function in synaptic and behavioural memory. *Nat Reviews* **3**:175-190

Lisman JE & Zhabotinsky AM (2001). A model of synaptic memory: a CaMKII/PP1 switch that potentiates transmission by organizing an AMPA receptor anchoring assembly. *Neuron* **31**:191-201.

Lledo PM, Zhang X, Sudhof TC, Malenka RC & Nicoll RA (1998) Postsynaptic membrane fusion and long-term potentiation. *Science* **279**:399-403.

Lu W-Y, Man H-Y, Ju W, Trimble WS, MacDonald JF & Wang YT (2001). Activation of synaptic NMDA receptors includes membrane insertion of new AMPA receptors and LTP in cultured hippocampal neurons. *Neuron* **29**:243-254.

Lüscher C, Xia H, Beattie EC, Carroll RC, von Zastrow M, Malenka RC, Nicoll RA (1999) Role of AMPA receptor cycling in synaptic transmission and plasticity. *Neuron* **24**:649-58.

Lüthi A, Chittajallu R, Duprat F, Palmer MJ, Benke TA, Kidd FL, Henley JM & Isaac JTR (1999). Hippocampal LTD expression involves a pool of AMPARs regulated by the NSF-GluR2 interaction. *Neuron* **24**:389-399.

Mack V, Burnashev N, Kaiser KMM, Rozov A, Jensen V, Hvalby Ø, Seeburg PH, Sakmann B & Sprengel R (2001). Conditional restoration of hippocampal synaptic potentiation in GluR-A-deficient mice. *Science* **292**:2501-2504.

Magee JC & Cook EP (2000). Somatic EPSP amplitude is independent of synapse location in hippocampal pyramidal neurons. *Nature Neurosci* **3:**895-903.

Magee JC & Johnston D (1997) A synaptically controlled, associative signal for Hebbian plasticity in hippocampal neurons. *Science* **275**:209-223.

Magee JC (1998) Dendritic hyperpolarization-activated currents modify the integrative properties of hippocampal CA1 pyramidal neurons. *J Neurosci.* **18**:7613-7624

Magee JC (2000). Dendritic integration of excitation synaptic input. *Nature Rev Neurosci* **1**:181-190.

Magee JC, Avery R, Christie BR, Johnston D (1996) Dihydropyridine-sensitive, voltage-gated Ca^{2+} channels contribute to the resting intracellular Ca^{2+} concentration of hippocampal CA1 pyramidal neurons. *J Neurophysiol* **76**:3460-3470.

Magee JC, Hoffman D, Colbert C, Johnston D (1998) Electrical and calcium signaling in dendrites of hippocampal pyramidal neurons. *Annu Rev Physio.* **60**:327-346.

Magee JC, Johnston D (1995) Characterization of single voltage-gated Na^{+} and Ca^{2+} channels in apical dendrites of rat CA1 pyramidal neurons. *J Physiol* **487**:67-90.

Magee JC. Christofi G, Christie B.R. & Johnston D. (1995) Subthreshold Ca^{2+} influx mediated through LVA calcium channels in the dendrites of CA1 pyramidal neurons. *J. Neurophysiol.* **74**:1335-1342.

Maletic-Savatic M, Koothan T & Malinow R (1998) Calcium-evoked dendritic exocytosis in cultured hippocampal neurons. Part II: Mediation by calcium/calmodulin-dependent protein kinase II. *J. Neurosci.* **18**:6814-6821.

Malinow R, Mainen ZF & Hayashi Y (2000) LTP mechanisms: from silence to four-lane traffic. *Curr Opin Neurobiol*. **10**:352-357.

Mammen A, Kameyama K, Roche KW, Huganir RL (1997) Phosphorylation of the α-amino-3-hydroxy-5-methylisoxazole-4-proprionic acid receptor GluR1 subunit by calcium/calmodulin-dependent kinase II. *J Biol Chem* **272**:32528-32533.

Mammen AL, Huganir RL & O'Brien RJ (1997) Redistribution and stabilization of cell surface glutamate receptors during synapse formation. *J Neurosci*. **17**:7351-7358.

Martin LJ, Blackstone CD, Levey AI, Huganir RL & Price DL (1993). AMPA glutamate receptor subunits are differentially distributed in rat brain. *Neuroscience* **53**:327-358.

Matsuzaki M, Ellis-Davies GC, Nemoto T, Miyashita Y, Iino M & Kasai H (2001). Dendritic spine geometry is critical for AMPA receptor expression in hippocampal CA1 pyramidal neurons. *Nature Neurosci* **4**:1086-1092.

Megias M, Emri Z, Freund TF & Gulyas AI (2001) Total number and distribution of inhibitory and excitatory synapses on hippocampal CA1 pyramidal cells. *Neuroscience* **102**:527-540.

Meng Y, Zhang Y & Jia Z (2003) Synaptic transmission and plasticity in the absence of AMPA glutamate receptor GluR2 and GluR3. *Neuron* **39**:163-76.

Molnár E & Isaac JTR (2002) Developmental and activity dependent regulation of ionotropic glutamate receptors at synapses. *ScientificWorldJournal* **2**:27-47.

Mosbacher J, Schoepfer R, Monyer H, Burnashev N, Seeburg PH & Ruppersberg JP (1994). A molecular determinant for submillisecond desensitization in glutamate receptors. *Science* **266**:1059-1062.

Nishimune A, Isaac JTR, Molnar E, Noel J, Nash SR, Tagaya M, Collingridge GL, Nakanishi S & Henley JM (1998). NSF binding to GluR2 regulates synaptic transmission. *Neuron* **21**:87-97.

Nusser Z, Lujan R, Laube G, Roberts JD, Molnar E, Somogyi P (1998) Cell type and pathway dependence of synaptic AMPA receptor number and variability in the hippocampus. *Neuron* **21**:545–559.

O'Brien RJ, Kamboj S, Ehlers MD, Rosen KR, Fischbach GD & Huganir RL (1998) Activity-dependent modulation of synaptic AMPA receptor accumulation. *Neuron* **21**:1067-78.

Passafaro M, Piech V & Sheng M (2001). Subunit-specific temporal and spatial patterns of AMPA receptor exocytosis in hippocampal neurons. *Nature Neurosci* **4**:917-926.

Petralia RS & Wenthold RJ (1992). Light and electron immunocytochemical localization of AMPA-selective glutamate receptors in the rat brain. *J Comp Neurol* **318:**329-354.

Pettit DL, Agustine GJ (2000) Distribution of functional glutamate and GABAReceptors on hippocampal pyramidal cells and interneurons. *J Neurophysiol* **84**:28-38.

Piccini A & Malinow R (2002). Critical postsynaptic density 95/disc large/zonula occludens-1 interactions by glutamate receptor 1 (GluR1) and GluR2 required at different subcellular sites. *J Neurosci* **22**:5387-5392.

Pickard L, Noel J, Henley JM, Collingridge GL & Molnár E (2000) Developmental changes in synaptic AMPA and NMDA receptor distribution and AMPA receptor subunit composition in living hippocampal neurons. *J Neurosci* **20**:7922-7931.

Poncer JC, Esteban JA, &Malinow R (2002) Multiple mechanisms for the potentiation of AMPA receptor-mediated transmission by alpha-Ca2+/calmodulin-dependent protein kinase II. *J Neurosci.* **22**:4406-4411.

Prange O, Murphy TH (1999) Analysis of multiquantal transmitter release from single cultured cortical neuron terminals. *J Neurophysiol* **81**:1810-1818.

Rall, W. Theory of physiological properties of dendrites. *Ann. NY Acad. Sci.* **96**:1071 (1962).

Reisel D, Bannerman DM, Schmitt WB, Deacon RM, Flint J, Borchardt T, Seeburg PH & Rawlins JNP (2002). Spatial memory dissociations in mice lacking GluR1. *Nature Neurosci* **5**:868-873.

Roche KW, Tingley WG, Huganir RL (1994) Glutamate receptor phosphorylation and synaptic plasticity. *Curr Opin Neurobiol* **4**:383-388.

Rosenmund C, Feltz A, Westbrook GL (1995) Synaptic NMDA receptor channels have a low open probability. *J Neurosci* **15(4):**2788-2795.

Royer S, Paré D, (2003) Conservation of total synaptic weight through balanced synaptic depression and potentiation. *Nature* **422**: 518-522.

Schikorski T, Stevens CF (1999) Quantitative fine-structural analysis of olfactory cortical synapses. *Proc Natl Acad Sci* **96**:4107-4112.

Scoville, WB, Milner, B. (1957) Loss of recent memory after bilateral hippocampal lesions. *J. Neuro. Psychiatry* **20**:11-21.

Shi S-H, Hayashi Y, Esteban JA & Malinow R (2001). Subunit-specific rules governing AMPA receptor trafficking to synapses in hippocampal pyramidal neurons. *Cell* **105**:331-343.

Sigworth FJ (1980) The variance of sodium current fluctuations at the node of ranvier. *J Physiol* **307**:97-129.

Silver AR, Cull-Candy SG, Takahashi T (1996) Non-NMDA glutamate occupancy and open probability at a rat cerebellar synapse with single and multiple release sites. *J Physiol* **494.1**:231-250.

Smart TG (1997) Regulation of excitatory and inhibitory neurotransmitter-gated ion channels by protein phosphorylation. *Curr Opin Neurobiol* **7**:358-367.

Smith MA, Ellis-Davies GCR & Magee JC (2003). Mechanism of the distance-dependent scaling of Schaffer collateral synapses in rat CA1 pyramidal neurons. *J Physiol* **548**:245-258.

Soderling TR, Tan SE, McGlade-McCulloh E, Yamamoto H, Fukunaga K (1994) Excitatory interactions between glutamate receptors and protein kinases. *J Neurobiol* **25**:304-311.

Song I & Huganir RL (2002) Regulation of AMPA receptors during synaptic plasticity. *Trends in Neurosci* **25**:578-588.

Sorra KE, Harris KM (1993) Occurrence and three dimensional structure of multiple synapses between individual radiatum axons and their target pyramidal cells in hippocampal area CA1. *J Neurosci* **13**:3736-3747.

Spruston N, Jonas P, Sakmann B (1995) Dendritic glutamate receptor channels in rat hippocampal CA3 and CA1 pyramidal neurons. *J Physiol* **482.2**:325-352

Sticker C, Fiel, AC, Redman SJ (1996) Statistic analysis of amplitude fluctuations in EPSCs evoked in rat CA1 pyramidal neurones in vitro. *J. Physiol (Lond)* **490**:419-441.

Sur C, Triller A, Korn H (1995) Morphology of the release site of inhibitory synapses on the soma and dendrite of an identified neuron. *J Comp Neurology* **351**:247-260.

Swanson GT, Kamboj SK & Cull-Candy SG (1997). Single-channel properties of recombinant AMPA receptors depend on RNA editing, splice variation, and subunit composition. *J Neurosci* **17**:58-69

Tachibana M, Wenthold RJ, Morioka H & Petralia RS (1994). Light and electron immunocythochemical localization of AMPA-selective glutamate receptors in the rat spinal cord. *J Comp Neurol* **344**:431-454.

Takumi Y, Ramírez-León1 V, Laake P, Rinvik E, Ottersen OP (1999) Different modes of expression of AMPA and NMDA receptors in hippocampal synapse. *Nature Neurosci* **2**:618 – 624.

Tao-Cheng JH, Vinade L, Pozzo-Miller LD, Reese TS & Dosemeci A (2001) Calcium/calmodulin-dependent protein kinase II clusters in adult rat hippocampal slices. *Neurosci* **115**:435-40.

Tardin C, Cognet L, Bats C, Lounis B & Choquet D (2003) Direct imaging of lateral movements of AMPA receptors inside synapses. *EMBO J*. **22**:4656-4665.

Tovar KR, Westbrook GL. (2002) Mobile NMDA receptors at hippocampal synapses. *Neuron* **34**:255-264.

Triller A, Seitanidou T, Franksson O & Korn H (1990). Size and shape of glycine receptor clusters in a central neuron exhibit a somato-dendritic gradient. *New Biol* **2**:637-641.

Trommald M, Jensen V, Andersen P (1995) Analysis of dendritic spines in rat CA1 pyramidal cells intracellularly filled with a fluorescent dye. *J Comp Neurol* **353(2):**260-274.

Trussell LO (1999). Synaptic mechanisms for coding timing in auditory neurons. *Annu Rev Physiol* **61**:477.

Turrigiano GG, Nelson SB (2000). Hebb and homeostasis in neuronal plasticity. *Curr Opin Neurobiol* **10**:358-364.

Turrigiano GG, Leslie KR, Desai NS, Rutherford LC & Nelson S (1998). Activity-dependent scaling of quantal amplitude in neocortical neurons. *Nature* **391**:892-896.

van Rossum MCW, Bi GQ & Turrigiano GG (2000). Stable hebbian learning from spike timing-dependent plasticity. *J Neurosci* **20**:8812-8821.

Verdoorn TA, Burnashev N, Monyer H, Seeburg PH & Sakmann B (1991). Structural determinants of ion flow through recombinant glutamate receptor channels. *Science* **252**:1715-1718.

Wang JH & Kelly PT (1997) Postsynaptic calcineurin activity downregulates synaptic transmission by weakening intracellular Ca2+ signaling mechanisms in hippocampal CA1 neurons. *J Neurosci.* **17**:4600-4611.

Wang JH &Kelly PT (1995) Postsynaptic injection of CA2+/CaM induces synaptic potentiation requiring CaMKII and PKC activity. *Neuron* **15**:443-452.

Wenthold RJ, Petralia RS, Blahos II J & Niedzielski AS (1996). Evidence for multiple AMPA receptor complexes in hippocampal CA1/CA2 neurons. *J Neurosci* **16**:1982-1989.

Williams SR & Stuart GJ (2002). Dependence of EPSP efficacy on synapse location in neocortical pyramidal neurons. *Science* **295**:1907-1910.

Xie X, Liaw JS, Baudry M, Berger TW (1997) Novel expression mechanism for synaptic potentiation: alignment of presynaptic release site and postsynaptic receptor. *Proc Natl Acad Sci U S A* **94**:6983-6988.

Yasuda H, Barth AL, Stellwagen D & Malenka RC (2003) A developmental switch in the signaling cascades for LTP induction. *Nat Neurosci* **6**:15-16.

Zamanillo D, Sprengel R, Hvalby Ø, Jensen V, Burnashev N, Rozov A, Kaiser KMM, Köster HJ, Borchardt T, Worley P, Lübke J, Frotscher M, Kelly PH, Sommer B, Andersen P, Seeburg PH & Sakmann B (1999). Importance of AMPA receptors for hippocampal synaptic plasticity but not for spatial learning. *Science* **284**:1805-1811.

Zhu JJ, Esteban JA, Hayashi Y & Malinow R (2000) Postnatal synaptic potentiation: delivery of GluR4-containing AMPA receptors by spontaneous activity. *Nat Neurosci* **3**:1098-1106.